Check for updates

Secondary structures in synthetic polypeptides from *N*-carboxyanhydrides: design, modulation, association, and material applications

Ziyuan Song, [ID] †[a] Hailin Fu, [ID] †[b] Ruibo Wang, [ID] [a] Lazaro A. Pacheco, [ID] [a] Xu Wang,[ac] Yao Lin [ID] *[b] and Jianjun Cheng [ID] *[a]

Synthetic polypeptides derived from the ring-opening polymerization of *N*-carboxyanhydrides can spontaneously fold into stable secondary structures under specific environmental conditions. These secondary structures and their dynamic transitions play an important role in regulating the properties of polypeptides in self-assembly, catalysis, polymerization, and biomedical applications. Here, we review the current strategies to modulate the secondary structures, and highlight the conformation-specific dynamic properties of synthetic polypeptides and the corresponding materials. A number of mechanistic studies elucidating the role of secondary structures are discussed, aiming to provide insights into the new designs and applications of synthetic polypeptides. We aim for this article to bring to people's attention synthetic polymers with ordered conformations, which may exhibit association behaviors and material properties that are otherwise not found in polymers without stable secondary structures.

[a] Department of Materials Science and Engineering, University of Illinois at Urbana-Champaign, Urbana, Illinois 61801, USA. E-mail: jianjunc@illinois.edu

[b] Department of Chemistry and Polymer Program at the Institute of Materials Science, University of Connecticut, Storrs, Connecticut 06269, USA. E-mail: yao.lin@uconn.edu

[c] Tianjin Key Laboratory on Technologies Enabling Development of Clinical Therapeutics and Diagnostics (Theranostics), School of Pharmacy, Tianjin Medical University, Tianjin 300070, P. R. China

† The authors contributed equally to this work.

1 Introduction

As one of the most important macromolecules for life, proteins have fascinated scientists for centuries. Throughout nature, proteins have been constructed for numerous biological functions including catalysis, cell support, and signal transduction.[1] Since the discovery of α-helices and β-sheets,[2,3] people realized that these secondary structures are the fundamental building blocks of nearly all proteins, regardless of their sequence and side chain structures. The formation of secondary structures and

Ziyuan Song received his BS degree in Materials Chemistry in 2011 from Peking University, China; and his PhD degree in Materials Science and Engineering in 2017 (working under Prof. Jianjun Cheng) from the University of Illinois at Urbana–Champaign. He is currently a postdoctoral associate in Prof. Jianjun Cheng's laboratory in the Department of Materials Science and Engineering, University of Illinois at Urbana–Champaign. His research interests include the design and conformational study of functional polypeptides for biomedical applications.

Ziyuan Song

Hailin Fu received her BS degree from the School of Chemistry and Chemical Engineering, Nanjing University, in 2012. She is currently a PhD student in Prof. Yao Lin's group at the Institute of Material Science, University of Connecticut. Her research interest includes nucleation induced cooperative behavior in the synthesis, conformational change, and self-assembly of complex macromolecular systems.

Hailin Fu

This journal is © The Royal Society of Chemistry 2018

Chem. Soc. Rev., 2018, 47, 7401–7425 | 7401

their three-dimensional arrangement in space (*i.e.*, tertiary structures) play a critical role in controlling the properties of proteins. In addition, conformational changes in response to changes in the environment are directly associated with the functioning of proteins.[4] For instance, calmodulin, a ubiquitous Ca^{2+}-dependent messenger protein, plays a tremendous role in regulating numerous intercellular processes.[5] Upon Ca^{2+} binding, calmodulin changes its structure from a "closed" conformation to an "open" conformation, leading to the exposure of its hydrophobic surfaces that bind to and regulate target proteins.[6]

Inspired by these proteins, researchers have developed various peptidomimetic oligomers or polymers, aiming not only to reconstruct these secondary structures through chemical synthesis, but also, more importantly, to control material properties by the manipulation of their secondary structures. These peptidomimetic materials, with α-peptide, β-peptide,[7,8] and peptoid backbone structures,[9–11] can adopt stable secondary structures when their side chains and sequences are properly designed. For instance, studies on peptidomimetic foldamers, which are beyond the scope of this review article, have shown us how scientists are able to modulate the conformation of a molecule through the variation of backbone building blocks, side-chain interactions, and the surrounding environment.[12–15]

Among various peptidomimetic materials, oligo(α-peptide)s and poly(α-peptide)s (usually written as oligopeptides and polypeptides) are most studied since they have the same backbone structure as natural proteins (*i.e.*, peptide bonds). These peptide-mimetic materials with ordered secondary structures, including α-helices and β-sheets, exhibit completely different self-assembly behaviors, biomedical performance, and catalytic activities from their random-coiled analogues. While the material properties of conventional synthetic polymers which exhibit no stable secondary structures are mainly regulated through the tuning of their degree of polymerization (DP), side-chain structures, and chemical compositions, synthetic polypeptides add an
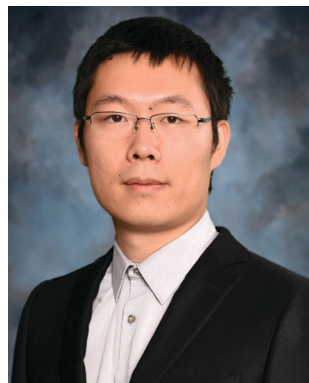
Ruibo Wang received his BS degree in Chemistry in 2013 from Peking University, China. He is currently a PhD student in Prof. Jianjun Cheng's laboratory in the Department of Materials Science and Engineering, University of Illinois at Urbana–Champaign. His research interests include the design and synthesis of functional polymers for biomedical applications.

Ruibo Wang

Lazaro Pacheco received his BS and MS degrees in Materials Science and Engineering from Rutgers University and Johns Hopkins University, respectively. He is now a PhD student in Materials Science and Engineering working under Prof. Jianjun Cheng at the University of Illinois at Urbana–Champaign. His research interest includes the synthesis of novel biomedically relevant polypeptides.

Lazaro A. Pacheco

Yao Lin obtained his BS degree in Macromolecular Science in 1995 from Fudan University, China; his MS degree in Chemistry in 2000 from the College of William and Mary; and his PhD degree in Polymer Science and Engineering in 2005 from the University of Massachusetts, Amherst. After completing his George W. Beadle postdoctoral fellowship at the Argonne National Laboratory and the University of Chicago in the fields of biosciences and chemistry, he joined the faculty at the University of Connecticut in late 2008. He took a sabbatical at the Institute of Complex Molecular Systems at the Eindhoven University of Technology in 2015. Yao Lin is currently an Associate Professor of the Chemistry and Polymer Program at the Institute of Materials Science at the University of Connecticut, Storrs.

Yao Lin

Jianjun Cheng obtained his BS degree in Chemistry in 1993 from Nankai University, China; his MS degree in Chemistry in 1996 from Southern Illinois University at Carbondale; and his PhD degree in Materials Science in 2001 from the University of California, Santa Barbara. He worked as a Senior Scientist at Insert Therapeutics, Inc., from 2001 to 2004 and did his postdoctoral research at MIT from 2004 to 2005. Jianjun Cheng is currently a Hans Thurnauer Professor of Materials Science and Engineering, and a faculty affiliate with the Beckman Institute for Advanced Science and Technology, Frederick Seitz Materials Research Laboratory, Department of Chemistry, Department of Bioengineering, Micro and Nanotechnology Laboratory, and Carl R. Woese Institute for Genomic Biology at the University of Illinois at Urbana–Champaign.
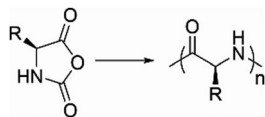
Jianjun Cheng

Fig. 1   Synthetic route to polypeptides from ring-opening polymerization of *N*-carboxyanhydrides.

extra parameter to modulate their functions and behaviors by controlling the conformation of the polymers. Currently, there are mainly three methods to prepare oligopeptide and polypeptide materials, namely solid phase peptide synthesis (SPPS),[16] microbial synthesis,[17] and ring-opening polymerization (ROP) of *N*-carboxyanhydrides (NCAs) (Fig. 1).[18] While the former two methods are able to produce monodisperse peptide materials with controlled sequences, microbial synthesis is typically used for the preparation of peptides bearing only natural amino acid residues, and SPPS is limited to short peptides (< 50 residues) and requires tedious procedures while suffering from low yields. On the other hand, although the NCA polymerization approach generates polydisperse polypeptides without precise sequence control, it offers considerable chemical diversity beyond the twenty-one natural amino acids and enables the large scale synthesis of high molecular weight (MW) polypeptides with various architectures. With the recent development of living NCA polymerization and functionalized NCA monomers, researchers can easily vary the polypeptide chain lengths and introduce versatile side-chain structures, producing well-defined polypeptide materials with controlled secondary structures.

In this article, we focus on discussing the design, modulation, and application of the secondary structures of synthetic polypeptides prepared from NCA polymerization. A recently published paper on a similar topic by Bonduelle highlights the fundamental principles of polypeptide polymer structuring, and briefly reviews the application of polypeptides adopting stable secondary structures.[19] Structural details and the characterization of secondary structures were already summarized in the said review, and thus will not be covered in this article. Herein, we aim to provide a comprehensive summary on the critical roles that secondary structures play in manipulating the performance of synthetic polypeptides. In addition, mechanistic studies elucidating the conformation-specific properties of synthetic polypeptides are highlighted, aiming to provide insights into the new design and application of polypeptide materials. We aim for this review article to serve as a complement to the existing library of review papers on synthetic polypeptides which mainly focused on NCA chemistry,[20] side-chain structure design,[21] self-assembly behaviors,[22,23] stimuli-responsive properties,[24,25] polypeptide-brushes on surfaces,[26,27] and biomedical applications.[23,28–33]

2 Modulation of secondary structures

In an attempt to elucidate the protein folding problem, the secondary structures, especially α-helices, of several proteins and their peptide segments were extensively studied in the late twentieth century.[34,35] The results suggest that the formation and stabilization of secondary structures are controlled not only by the intrinsic α-helix/β-sheet propensities of each amino acid residue, but also through specific interactions between the side chains of the peptides.[36] In addition, the impact of side-chain interactions on helix formation depends on the positions of the amino acid residues in the peptide sequence.[37] These studies provided valuable insights into the modulation of secondary structures in synthetic polypeptides obtained by the ROP of NCAs.

2.1   Impact of side-chain interactions on the conformations of synthetic polypeptides

Synthetic polypeptides, made by SPPS, microbial synthesis or NCA polymerization, are composed of both natural and non-natural amino acids derived by the functionalization of natural amino acids (*e.g.*, Glu, Lys, Ser, and Cys).[21] The α-helix/β-sheet propensities of these natural amino acids are therefore inadequate in predicting the secondary structures of these synthetic polypeptides. In addition, polypeptides derived by NCA polymerization are typically composed of fewer than four types of amino acid residues. Thus, several important side-chain interactions contributing to the stability of secondary structures in natural peptides, such as the Glu–Lys salt bridge[37] and hydrogen bonding (H-bonding) interactions of N-capping residues,[38] are not common in synthetic polypeptides. To date, the formation and stabilization of secondary structures in most developed synthetic polypeptide systems have been controlled by the interactions of one or two types of side chains, including coulombic interactions, hydrophobic interactions, and H-bonding interactions.

2.1.1   Side-chain coulombic interactions.
In peptides, coulombic attraction can either stabilize or destabilize the helical conformation depending on the spacing of the charged residues.[37] However, such attractive interactions are seldom observed in synthetic polypeptides with helical conformations due to the difficulty in accurately placing ion pairs at desired positions in a polymer chain. The major coulombic interactions in synthetic homopolypeptides are repulsive interactions, which make the α-helical conformation unstable, as observed in poly(L-glutamic acid)s (PLGs) at neutral or basic pH.[39] Once the charged groups of these polypeptides are shielded by protonation/deprotonation, the α-helical conformation is recovered. Similarly, charge-induced β-sheet–coil transitions have also been reported if the peptide residue has an intrinsic propensity to form β-sheets (*e.g.*, poly(*S*-carboxymethyl-L-cysteine)s).[40]

In random copolypeptides bearing both positive and negative side chains, attractive coulombic interactions commonly serve as destabilizing forces of the helical conformation, as the spacings of opposite charges are random.[41,42] On the other hand, the mixing of two polypeptide chains bearing opposite charges, such as PLG and poly(L-lysine) (PLL), results in the formation of polyion complexes (PICs) with a β-sheet conformation.[43,44] The formation of β-sheet structures requires both polypeptide chains to possess the same chirality, as the use of achiral polypeptides only gives rise to the formation of random-coiled PICs.[43]

2.1.2   Side-chain hydrophobic interactions.
Side-chain hydrophobic interactions favor the formation of ordered α-helical or

β-sheet conformations of synthetic polypeptides, in a similar manner to their peptide analogues.[45] Depending on their side-chain structures, hydrophobic homopolypeptides adopt either α-helical or β-sheet conformations. For instance, poly(L-leucine) (PLLeu) adopts a stable α-helical conformation,[46] while poly-(L-valine) (PLVal) prefers a β-sheet structure.[47]

In 1966, Berger and co-workers developed a series of poly-(N-(ω-hydroxyalkyl)-L-glutamine)s with different lengths of alkyl spacers, aiming to study the impact of side-chain hydrophobic interactions on the α-helical conformation.[48] The polypeptide with the longest spacer, poly(N-(4-hydroxybutyl)-L-glutamine), exhibited higher helicity and better helical stability than its analogues bearing shorter spacers, suggesting that hydrophobic interactions favor the formation and stabilization of α-helical structures. Similar trends were also observed in charged polypeptides[49] and glycopolypeptides.[50] Furthermore, replacing alkyl spacers with more hydrophobic aromatic linkers has been demonstrated to further stabilize α-helices in glycopolypeptides.[50] In an attempt to confirm the stabilization effect of side-chain hydrophobic interactions, the hydrophobicity of alkyl spacers was manipulated either by experimentally replacing some CH_2 units with an O atom,[49] or by artificially elevating the hydrophilicity of CH_2 groups in a simulation.[51] In both cases, the polypeptides with less hydrophobic spacers were unable to adopt stable α-helical structures.

2.1.3 Side-chain hydrogen bonding interactions. Although side-chain H-bonding interactions have been reported to stabilize α-helices in natural peptides,[37,52] these interactions have not been well studied in synthetic polypeptides. Recently, Cheng, Yin, Ferguson, and co-workers reported that the donor–acceptor patterns of side-chain H-bonding ligands have a profound impact on the formation of the secondary structures of synthetic polypeptides.[53] H-bonding ligands bearing both hydrogen bond (H-bond) donors and acceptors (referred to as a "binary H-bonding pattern", BHB), such as amides, disrupt the α-helical conformation when incorporated onto the side chains of polypeptides. In contrast, H-bonding ligands with only H-bond donors or acceptors (referred to as a "unitary H-bonding pattern", UHB) do not show obvious disruptive effects. Although the molecular mechanism was not clear, the authors suggested that the H-bonding interactions between backbone amides and side-chain BHB ligands play a critical role in disrupting the α-helical structures.

2.2 Design of α-helical, water-soluble polypeptides

Water-soluble polypeptides with α-helical conformations are of great importance for biomedical applications. In nature, such polypeptides are constructed by placing ionic groups on one side of the α-helix to maintain water solubility, and hydrophobic groups on the opposite side to stabilize the peptide's secondary structure.[54] Ionic groups can also help stabilize the α-helical conformation through the formation of salt bridges. This strategy, however, is not suitable for synthetic polypeptides since precise sequence control is difficult to achieve. Common water-soluble polypeptides including PLG and PLL, when in their charged forms, adopt

random coil conformations in water because of charge repulsion between side chains.

In order to solve this charge repulsion problem, scientists have come up with two strategies to prepare α-helical, water-soluble synthetic polypeptides. For the first strategy, non-ionic hydrophilic groups, such as oligo(ethylene glycol) (OEG)[55–59] and sugar units,[60] were incorporated into the side chains of polypeptides. These groups render the polypeptides water-soluble while limiting repulsive interactions that may potentially destabilize the formation of α-helices. As a result, OEG-containing polypeptides and glycopolypeptides have been demonstrated to adopt stable α-helical structures in aqueous solution (Fig. 2A).

In 2011, Cheng, Lin, and co-workers developed the first ionic polypeptides with stable α-helical conformations by extending the spacing of the charged functionality from the polypeptide backbone (Fig. 2B).[49] The decreased charge repulsion and the enhanced hydrophobic interactions resulted in good stability of α-helices against changes in pH and temperature, as well as the addition of denaturing reagents. Following this work, several cationic and anionic polypeptides adopting stable α-helical structures have been prepared.[41,61–65] A similar strategy was also employed to prepare ionic polypeptides with stable β-sheet conformations.[66]

2.3 Trigger-responsive helix–coil transitions

Synthetic polypeptides with α-helical conformations exhibit several beneficial properties compared with their random coiled analogues. Therefore, it is of great interest to design
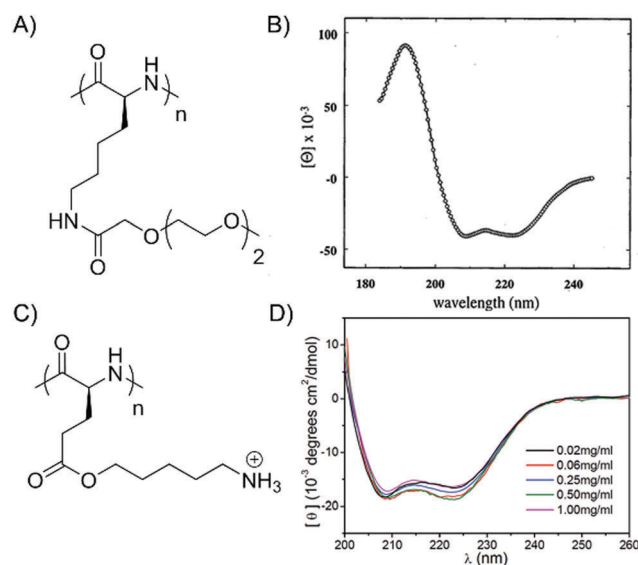

Fig. 2 Design of water-soluble, α-helical polypeptides. (A and B) Chemical structure (A) and CD spectrum (B) of a water-soluble, α-helical polypeptide bearing non-ionic side chains. Reprinted with permission from ref. 55. Copyright 1999 American Chemical Society. (C and D) Chemical structure (C) and CD spectra (D) of a water-soluble, α-helical polypeptide bearing elongated hydrophobic side chains with a charged terminus. The concentration-independent CD spectra indicate that the α-helices remain monomeric in aqueous solution. Reprinted with permission from ref. 49. Copyright 2011 Springer Nature. In both cases, the double-minimum curves at 208 and 222 nm on the CD spectra indicate α-helical conformations.

7404 | Chem. Soc. Rev., 2018, 47, 7401–7425

This journal is © The Royal Society of Chemistry 2018

trigger-responsive, conformationally switchable polypeptides, which can be "activated" (coil-to-helix) or "deactivated" (helix-to-coil) on demand. Here, we discuss three strategies which are used to design synthetic polypeptides with helix–coil transition behaviors. Some other conformationally switchable synthetic polypeptides, such as polypeptides with α-helix-to-β-sheet[67] or β-sheet-to-coil transitions,[40] will not be discussed in detail.

2.3.1 Manipulation of side-chain charges.
Learning from the well-known examples of PLG and PLL, the shielding/exposure of side-chain charges is the most commonly used strategy to modulate the secondary structures of synthetic polypeptides. For example, PLG adopts a typical random coil structure when its side chains are charged. Once the charges are eliminated through protonation,[68,69] esterification,[41,70] metal coordination,[71] or salt screening,[72] recovery of the α-helical conformation is observed.

Considering the facile chemistry to attach various trigger-responsive moieties on the side chains of PLG, PLL, and poly-(L-cysteine) (PLCys), control of side-chain charges is the most versatile strategy to design synthetic polypeptides with helix–coil transition behaviors.[41,70,73–77] For instance, the nitro-benzyl functionality and its derivatives are widely used in the design of UV-responsive polypeptide materials. As shown in Fig. 3A, poly(γ-(4,5-dimethoxy-2-nitrobenzyl)-L-glutamate) (PDMNBLG) gradually loses its helical structure upon UV irradiation due to the deprotection of PLG groups.

2.3.2 Manipulation of side-chain polarity.
Deming and co-workers reported the redox-responsive helix–coil transition of PLCys derivatives, which exhibited a helix-to-coil transition once the side-chain thioethers were oxidized to sulfones.[78] The change in the secondary structure was attributed to the increase of side-chain polarity, since the polar sulfone groups were likely to disrupt the hydrophobic interactions between side chains through their interaction with water.

Following this work, the authors further developed synthetic polypeptides with reversible helix–coil transition behaviors.[74] When sugar- or OEG-based poly(L-homocysteine) derivatives were used, the controlled oxidation of side-chain thioether groups to sulfoxide groups led to a change in the secondary structure to random coil. Interestingly, the side-chain sulfoxides
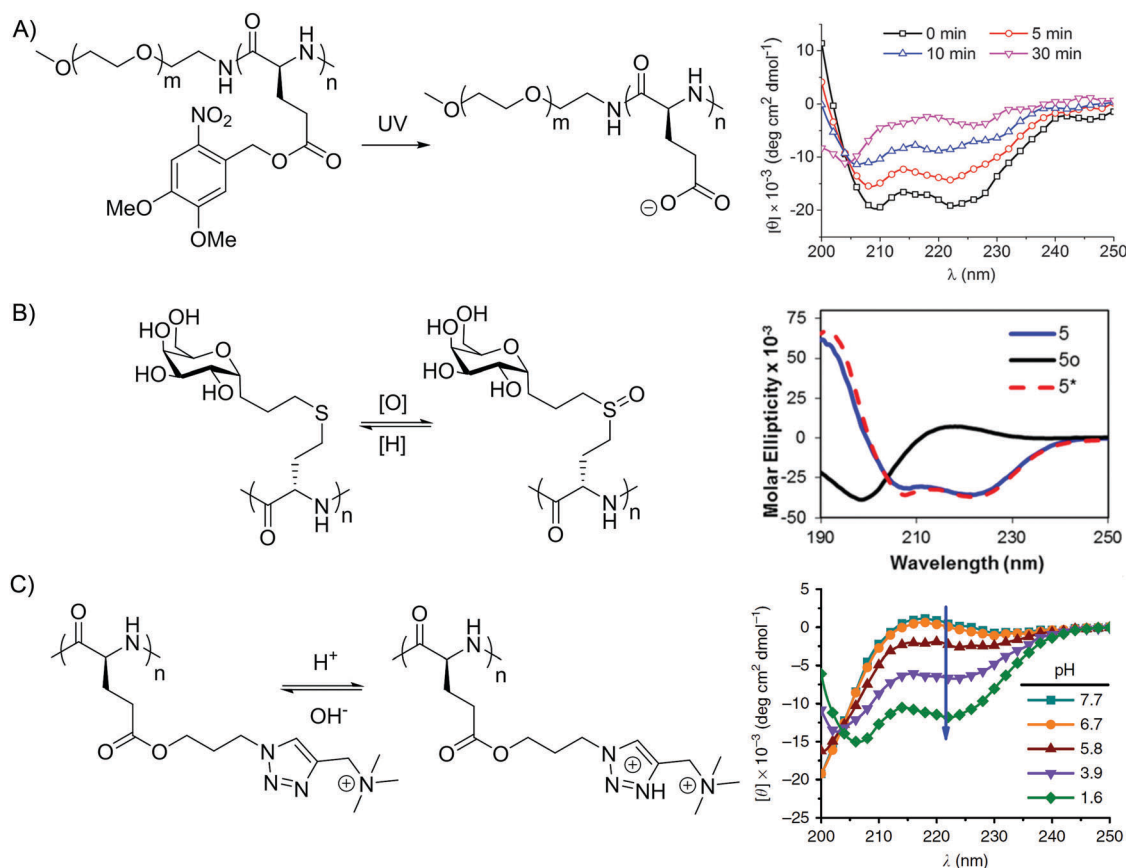

Fig. 3 Trigger-responsive helix–coil transition of polypeptides. (A) Chemical structure and UV-triggered helix-to-coil transition of PDMNBLG. Upon UV irradiation, the cleavage of side-chain esters leads to the exposure of negative charges, which destabilizes the α-helical conformation due to charge repulsion. Reprinted with permission from ref. 70. Copyright 2015 Royal Society of Chemistry. (B) Chemical structure and redox-responsive, reversible helix–coil transition of sugar-based poly(L-homocysteine) derivatives. The oxidation of side-chain thioethers to sulfoxides increases the polarity and disrupts the hydrophobic interaction of side chains, resulting in a helix-to-coil transition. 5 was first oxidized to 5o, which was then reduced back to 5*. Reprinted with permission from ref. 74. Copyright 2014 American Chemical Society. (C) Chemical structure and pH-responsive, reversible helix–coil transition of triazole-based polypeptides. The protonation/deprotonation of side-chain triazoles alters their hydrogen bonding pattern, leading to reversible conformational changes of the polypeptides. Reprinted with permission from ref. 53. Copyright 2017 Springer Nature.

can be reduced back to thioethers with the addition of thioglycolic acid, reversing the change in the secondary structure (Fig. 3B).

2.3.3   Manipulation of side-chain H-bonding. The impact of side-chain H-bonding patterns on secondary structures was also applied in the design of polypeptides with helix–coil transition properties.[53] 1,2,3-Triazole was introduced into the side chains of polypeptides as a modulator, whose H-bonding pattern was controlled by aqueous pH. Under acidic conditions, the BHB pattern triazole groups were protonated into a UHB pattern triazolium, resulting in the recovery of α-helices (Fig. 3C). The reversibility of the helix–coil transition was conclusively demonstrated with both experimental and simulation-based methods.

2.4   Nonlocal interactions in the helix–coil transition of polypeptide-containing macromolecules in solution

The classic statistical mechanical models for helix–coil transition, which were developed by Schellman,[79] Gibbs,[80] Zimm,[81] Lifson,[82] and Nagai,[83] are all based on local interactions and consider neither inter-chain nor intra-chain nonlocal interactions. In most cases, the nonlocal interactions were found to be able to disrupt the persistence of helical rods. In both the bulk state and concentrated solutions,[84,85] it is found that there are strong inter-chain or intra-chain nonlocal interactions that disrupt α-helices into "broken rods" instead of a single intact rod. In dilute solutions, this could also be the case when local proximity is realized by the grafting of side chains onto brush polymers[86] or the folding of long, linear polypeptides.[87] Lin, Cheng, and co-workers systematically explored the helix-to-coil transition behavior of poly(γ-benzyl-L-glutamate) (PBLG) and polynorbornene-g-PBLG (PN-g-PBLG) in CDCl₃ with different fractions of trifluoroacetic acid (TFA).[88] It was shown that the transition sharpness (i.e., the apparent cooperativity) decreases as the grafting density increases in the randomly grafted brush polymer (Fig. 4A), indicating a greater tendency for the α-helical rod to break into shorter segments as the side chains become closer to each other. In nuclear Overhauser enhancement

spectroscopy (NOESY) experiments, it was found that the normalized off-diagonal cross peak intensity is inversely correlated with the normalized apparent cooperativity, suggesting that the intensity of nonlocal interactions controls the folding behaviors of the polypeptide chains in the crowding environment.

Due to the existence of nonlocal interactions, considerable deviations from the classic models may be observed in the polypeptide-containing macromolecules with complex architectures, or polypeptides with large DPs. Lin, Cheng, and co-workers[86] analyzed the helix–coil transition behavior of poly(ε-benzyloxycarbonyl-L-lysine)s (PZLLs) and PN-g-PZLLs at different temperatures and different solvents with the Schellman–Zimm–Bragg model.[86] It was found that while Schellman's model explains the helix–coil transition behaviors of the linear PZLLs (the DP ranges from 35 to 150) in CDCl₃ fairly well, it could not fit the helix–coil transition curves of the brush polymer PN-g-PZLLs. The same team also investigated the folding behaviors of linear polypeptides (e.g., PBLGs) with very high DPs.[87] They found that while Zimm–Bragg model can describe the helix-coil transition of short PBLGs, the prediction from the model deviates significantly from the experiments when the chains have a DP above 300 (Fig. 4B), presumably due to the interactions among the different helical segments in a long chain.

As the classic models have difficulties in accurately describing the helix-to-coil transitions in comb- or brush-like polymers and long, linear polypeptides, there arose a need for new models which consider non-local interactions. Ghosh and Dill first developed a model that considers non-local interactions in multi-bundle protein folding.[89] On the basis of Schellman's model, the authors further considered the cases where there are two or three helices within a single chain, and incorporated the term of nonlocal interactions between the helix bundles by treating the hydrophobic and van der Waals interactions between helices as a binding equilibrium. The model is shown to be able to predict the thermal and urea induced helix–coil transitions correctly for single helix and three-helix-bundled proteins. Following this approach, Lin, Cheng, and co-workers modified Ghosh–Dill's model and applied it to the analysis of the helix–coil transition behavior of brush polymer PN-g-PZLL, and obtained good agreement between the theoretical predictions and experimental results.[86]

3 The role of secondary structures in self-assembly in solution

Proteins are generally composed of 21 natural amino acids, while in polypeptides both natural and non-natural amino acids can be included. This versatility in side chain functionality, along with the flexible design of the molecular topology, enables more diverse folding and self-assembly behaviors, post-modulation methods, and environmental responsiveness in both aqueous and organic solutions. The diversity in self-assembled structures, viability for in situ structural control, and biocompatibility make synthetic polypeptides good
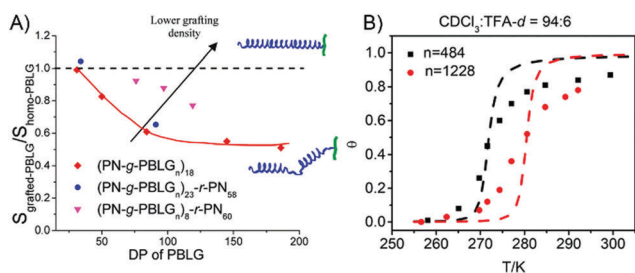

Fig. 4 Nonlocal interactions in helix−coil transitions. (A) plot of $S_{grafted-PBLG}$/$S_{homo-PBLG}$ as a function of the DP of grafted-PBLG chains. $S_{grafted-PBLG}$/$S_{homo-PBLG}$ represents the normalized apparent cooperativities of grafted-PBLGs, and is strongly dependent on grafting density. Reprinted with permission from ref. 88. Copyright 2011 American Chemical Society. (B) Temperature-induced helix−coil transition of PBLG with two different lengths at CDCl₃ : TFA-d = 94 : 6 (v/v). θ stands for the average fractional helicity. Experimental results (shown as scattered symbols) deviate from the predictions of the Zimm−Bragg model (shown as dashed lines). Reprinted with permission from ref. 87. Copyright 2017 American Chemical Society.

7406 | Chem. Soc. Rev., 2018, **47**, 7401–7425

This journal is © The Royal Society of Chemistry 2018

candidates for drug delivery,[90–96] and applications in food[97] and cosmetics.[98]

The activities of proteins rely on their tertiary structure. Likewise, the application of polypeptides relies on their self-assembled structures which are guided and stabilized by their secondary structures. Desirable structures typically include coacervates,[99,100] vesicles,[70,90–96] gels,[44,101–103] and membranes.[93] Control of macroscopic self-assembly is realized by a delicate balance in hydrophilicity/hydrophobicity, charge interactions, secondary structure motif interactions, and other environmental factors. In this section, we will focus on how secondary structures influence and guide the self-assembly of polypeptides.

3.1 The role of α-helical rods in the formation of vesicles or sheet-like membranes

The use of polypeptide-based vesicles in drug delivery is largely appealing due to their multifunctionality and biomimetic nature, and the ability of polypeptides to adopt different secondary structures. α-Helical forming polypeptides are extremely efficient at anisotropic packing, which tends to favor the formation of vesicles or membranes.[90,91] In an amphiphilic diblock or triblock copolymer,[104] different morphologies have been achieved by balancing the packing of hydrophobic, α-helical blocks with coulombic repulsions from charged blocks[91,101] or hydrophilicity from nonionic blocks.[90,105,106] Generally, the morphologies of the assemblies are controlled by the fractions and relative lengths of the α-helical, hydrophobic, and vesicle-forming polypeptide segments.

Typically, block copolypeptides containing a long, hydrophilic, random coil block and a short, hydrophobic, α-helical block favor the formation of micelles[107] or gels[101] in water, while short, hydrophilic, random coil blocks combined with long, hydrophobic, α-helical blocks favor the formation of vesicles.[108] Deming and co-workers designed a series of amphiphilic diblock copolypeptides, PLL-*b*-PLLeu (named K_xL_y in the original paper) (Fig. 5A and B),[91] to systematically test the effects of the fraction of helices on the morphology of the self-assembled structures. Polypeptides with the largest fraction of α-helical blocks (PLL$_{20}$-*b*-PLLeu$_{20}$) formed membranes in aqueous environments (Fig. 5C). As the fraction of α-helical segments decreased, the self-assembled structure converted into fibrils (PLL$_{40}$-*b*-PLLeu$_{20}$, Fig. 5D), vesicles (PLL$_{60}$-*b*-PLLeu$_{20}$, Fig. 5E), and eventually irregular aggregates (PLL$_{80}$-*b*-PLLeu$_{20}$, Fig. 5F). When the chain length is increased while maintaining the same helical fraction (PLL$_{160}$-*b*-PLLeu$_{40}$ compared with PLL$_{80}$-*b*-PLLeu$_{20}$), the formation of gels was observed,[101] presumably due to stronger charge repulsions. In addition, a hydrophobic polypeptide segment with DP > 10 is critical for helix-directed self-assemblies, as shorter chains with DP < 10 are not able to form stable α-helices. Kamei, Deming, and co-workers demonstrated that while a vesicular morphology was mainly observed for PLL$_{60}$-*b*-PLLeu$_{20}$ and PLL$_{60}$-*b*-PLLeu$_{25}$, PLL$_{60}$-*b*-PLLeu$_{10}$ formed a mixture of micelles and vesicles, with the former being predominant.[109]

In addition to block copolypeptides bearing charged, hydrophilic blocks, Deming and coworkers reported the self-assembly behavior of poly(ε-2-(2-(2-methoxyethoxy)ethoxy)acetyl-L-lysine)
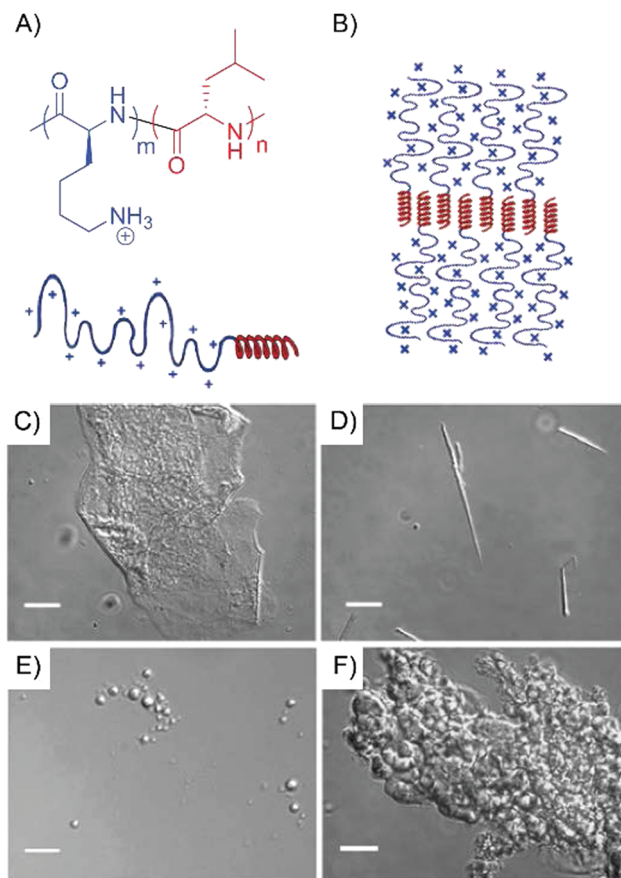

Fig. 5 The influence of the fraction of hydrophobic helices on the morphology of the self-assembled structure. (A and B) Chemical structure, schematic illustration (A), and proposed packing (B) of the PLL-*b*-PLLeu diblock polymers. The charged PLL segment adopts a random coil structure, and the hydrophobic PLLeu block folds into an α-helix. (C–F) Differential interference contrast (DIC) images of 1% (w/v) aqueous suspensions of PLL-*b*-PLLeu with various compositions. Scale bar = 5 μm. The fraction of helical segments in the PLL-*b*-PLLeu controls the morphology of the self-assembled structure. With decrease of the fraction of helical PLLeu blocks, the morphology changes from membranes (C, PLL$_{20}$-*b*-PLLeu$_{20}$), fibrils (D, PLL$_{40}$-*b*-PLLeu$_{20}$), and vesicles (E, PLL$_{60}$-*b*-PLLeu$_{20}$) to irregular aggregates (F, PLL$_{80}$-*b*-PLLeu$_{20}$). Reprinted with permission from ref. 91. Copyright 2005 American Chemical Society.

(PEG2LLys)-*b*-PLLeu (named $K^P_xL_y$ in the original paper), which bears a non-ionic, hydrophilic block (Fig. 6A and B).[90] Both the hydrophilic and hydrophobic segments are able to exhibit an α-helical conformation, resulting in the formation of sub-micrometer assemblies, vesicles (Fig. 6C), membrane structures (Fig. 6D), or irregular aggregates, depending on the chain lengths and the fraction of the hydrophobic blocks. The authors have shown that longer chains prefer the formation of membranes over vesicular structures at a fixed fraction of hydrophobic blocks (*e.g.*, PEG2LLys$_{200}$-*b*-PLLeu$_{40}$ formed membranes, while PEG2LLys$_{100}$-*b*-PLLeu$_{20}$ formed vesicles).

3.2 The role of secondary structures in gelation

Protein- and peptide-based hydrogels, which are typically formed by chemical or physical crosslinks,[110] are widely used
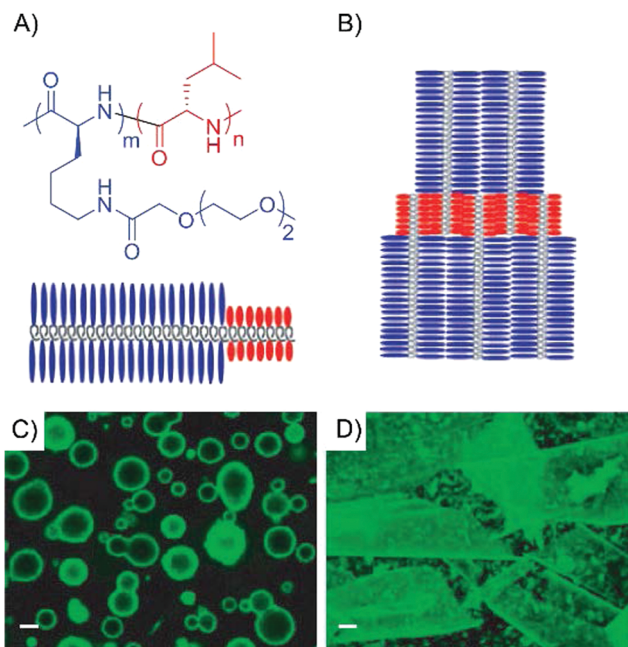
Fig. 6 The influence of the chain length on the morphology of the self-assembled structure. (A and B) Chemical structure, schematic illustration (A), and proposed packing (B) of the PEG2LLys-b-PLLeu diblock polymers. Both the hydrophobic PLLeu block and the hydrophilic, non-ionic PEG2LLys block adopt α-helical conformations. (C and D) Laser scanning confocal microscopy (LSCM) images of PEG2LLys$_{100}$-b-PLLeu$_{20}$ (C) and PEG2LLys$_{200}$-b-PLLeu$_{40}$ (D) visualized with DiOC$_{18}$ dye. Scale bar = 5 μm. With a fixed hydrophilic-to-hydrophobic ratio, the chain length dictates the morphology of the self-assembled structures, where shorter chains prefer the formation of vesicles (C) and longer chains prefer the formation of sheet-like membranes (D). Reprinted with permission from ref. 90. Copyright 2004 Springer Nature.

in food, cosmetics, drug delivery, and tissue engineering due to their tunable mechanical and structural properties, desired biodegradability, and good biocompatibility.[111,112] However, due to inconsistencies between materials extracted from natural sources, there is a call for the development of synthetic materials as replacements.[101] With their ability to form ordered secondary structures, synthetic polypeptides remain one of the most promising synthetic gel-forming materials. Besides hydrophobic interactions that are often used in random coil polymers as the association forces, synthetic polypeptides are able to make use of their conformation as another tunable handle. Helical rods have a strong preference to align with each other, and the formation of β-sheets is intrinsically accompanied by inter-chain H-bonding, both of which can be used as inter-chain crosslinks.

By exploiting these association forces as the inter-chain crosslinks and balancing them with charge repulsions, Deming and co-workers developed a series of diblock, triblock, and pentablock copolypeptides, aiming to study the impact of secondary structures on the gelation behavior.[101] PLL-b-PLLeu (Fig. 7A, polymer 1) and PLL-b-PLVal (Fig. 7A, polymer 2) were found to be able to form gels at concentrations as low as 0.25 wt% while maintaining their mechanical strength and a rapid recovery rate after stress at temperatures up to 90 °C. The rheological

behaviors of PLL$_{160}$-b-PLLeu$_{40}$, PLL$_{160}$-b-PLVal$_{40}$, and PLL$_{160}$-b-poly(DL-leucine)$_{40}$ (PDLLeu) (Fig. 7A, polymer 3), which adopts the α-helix, β-sheet, and random coil, respectively, were studied. Both the α-helical and β-sheet conformations promoted gelation, while the random coil conformation significantly increases the gelation threshold (from 0.25% to 2 wt%) (Fig. 7B). Replacing the PLL block with PLG did not significantly alter the rheological behavior (Fig. 7A, polymer 4), suggesting the critical role of the hydrophobic blocks in controlling the gelation. In addition, Jeong and co-workers demonstrated the enhanced gelation ability of β-sheets over the random coils by comparing the gelation behavior of poly(L-alanine) (PLAla)/poly(DL-alanine)(PDLAla)–poloxamer–PLAla/PDLAla[113] copolymers and PEG-b-PLAla/PDLAla[105] under physiologically relevant conditions. Schlaad and co-workers further confirmed the importance of ordered secondary structures by controlling the stereo-sequences of poly(ε-benzyl-oxycarbonyl-lysine) (PZLys).[106] Three PEG-b-PZLys with the same composition but different conformations were prepared (Fig. 7C), whose tendency to form gels follows the order of β-sheet > α-helix > random coil (Fig. 7D).
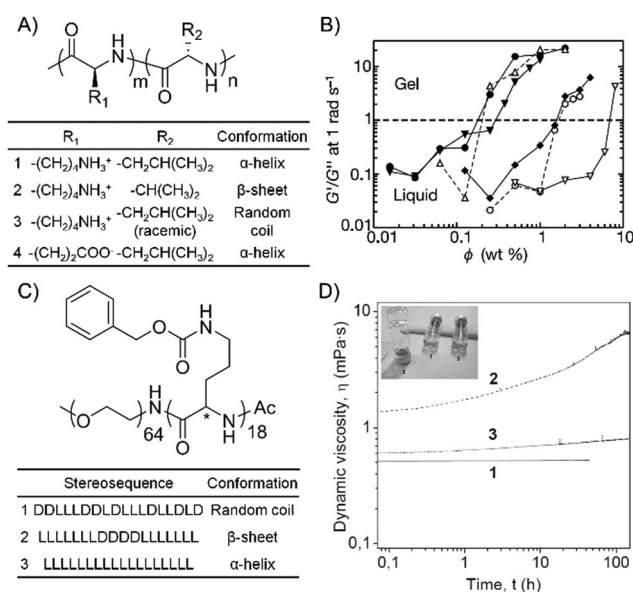

Fig. 7 The role of secondary structures in gelation. (A) The chemical structures and the conformations of PLL-b-PLLeu (1), PLL-b-PLVal (2), PLL-b-PDLLeu (3), and PLG-b-PLLeu (4). (B) The gelation behavior of the diblock polypeptides in A. Filled circles, PLL$_{160}$-b-PLLeu$_{40}$; open circles, PLL$_{180}$-b-PLLeu$_{20}$; filled down triangles, PLL$_{160}$-b-PLVal$_{40}$; open down triangles, PLL$_{180}$-b-PLVal$_{20}$; filled diamonds, PLL$_{160}$-b-PDLLeu$_{40}$; and open up triangles, PLG$_{160}$-b-PLLeu$_{40}$. Compared to those that exhibit α-helices (PLL-b-PLLeu and PLG-b-PLLeu) and β-sheets (PLL-b-PLVal), the diblock copolypeptide in the random coil state (PLL-b-PDLLeu) shows a much higher gelation threshold. Reprinted with permission from ref. 101. Copyright 2002 Springer Nature. (C) The chemical structures and conformations of three PEG-b-PZLys copolymers with different stereo-sequences. (D) Time-dependent evolution of the dynamic viscosity of THF solutions of the three PEG-b-PZLys samples with the photographs as the inset. The sample that forms β-sheets has the strongest tendency to form gels. Reprinted with permission from ref. 106. Copyright 2011 American Chemical Society.

7408 | Chem. Soc. Rev., 2018, 47, 7401–7425

This journal is © The Royal Society of Chemistry 2018

3.3 The role of secondary structures in coacervates

Charged polypeptides play an important role in generating coacervates, which are widely used in biomedical areas such as bone cement, deep tissue bonding, and drug encapsulation.[114,115] Coacervation is a type of electrostatically driven liquid–liquid phase separation that forms through the complexation of oppositely charged molecules.[116,117] The mixing of oppositely charged polyelectrolytes leads to either solid precipitates or liquid coacervate complexes, depending on the strength of the long-range electrostatic interactions.[118] Recently, Tirrell and co-workers reported that the short-range forces exerted by H-bonding were also a determining factor in phase selection.[43] In polypeptide-based PICs, inter-chain H-bonding and the formation of β-sheets led to solid precipitates, while coacervates formed when polypeptides adopt either the random coil or α-helical conformation.

When two oppositely charged polypeptides, poly(lysine) (PK) and poly(glutamic acid) (PE), were enantiomerically pure, β-sheets formed since the backbone alignment was facilitated by the electrostatic interactions (Fig. 8A).[43] This in turn enhanced the electrostatic interactions and further promoted the formation of solid precipitates (Fig. 8B). However, when at least one of the polypeptides (pK or pE) was racemic, the formation of β-sheets halted (Fig. 8A) and a liquid coacervate complex was formed instead (Fig. 8B), indicating that the formation of liquid coacervates is favored when a random coiled conformation is present.

In addition, Tirrell and co-workers reported the formation of liquid coacervates when mixing pE and a positively charged, α-helical polypeptide, poly(γ-3-(4-(guanidinomethyl)-1H-1,2,3-triazol-1-yl)propyl-L-glutamate) (PPLGPG).[100] The stable α-helical structure of PPLGPG forbade the formation of β-sheets (Fig. 8C), which would otherwise induce solid precipitates. The resulting coacervates exhibited enhanced resistance to salt dissolution compared with random coiled pK/PE coacervates, which was attributed to the higher charge density of helical polypeptides.

3.4 Topology and anti-parallel β-sheets

Until now, we have only concerned ourselves with linear polypeptides where only one or two sites on each peptide contributed to inter-chain interactions. However, proteins such as tubulin and actin are usually assembled through the interactions of multiple sites with directional and specific forces.[119,120] The self-assembly of tubulins and actins follows a cooperative manner and gives rise to much more complex and hierarchical structures.

In synthetic systems, these multi-site interactions are achievable with brush polymers which have multiple side chains connected in a covalent manner. In a recent work by Lin, Cheng, and co-workers, these multi-chain interactions were found to be able to enhance the formation of anti-parallel β-sheets, an important component for protein-based assemblies.[121] In this work, a comb polymer with an array of polypeptides (PN-g-PLG) was subjected to multivalent H-bonding, whose multi-chain interaction behavior in water was evaluated. Initially, the polymer was soluble and well dispersed with a partial coil and partial helix conformation at neutral pH. Due to the branched nature of
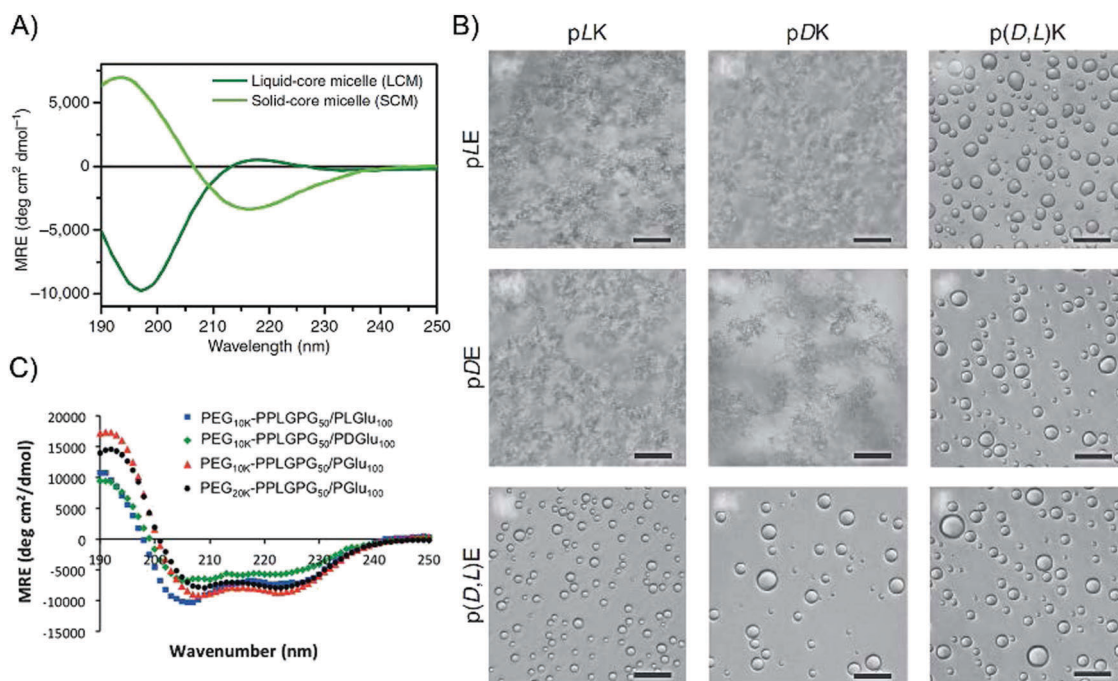

Fig. 8 The role of secondary structures in coacervates. (A) CD spectra of PEG-pLK + p(D,L)E (dark green) and PEG-pLK + pLE (light green). The mixing of racemic polymers prevents the formation of β-sheets. (B) Optical micrographs of polyelectrolyte complexes. Scale bar = 25 μm. The liquid coacervates are formed in the presence of at least one racemic polymer, i.e. without the formation of β-sheets. Reprinted with permission from ref. 43. Copyright 2015 Springer Nature. (C) CD spectra of PEG-PPLGPG + poly(glutamic acid)s. When charged polypeptides adopt stable α-helical conformations, the formation of β-sheets is also prevented, resulting in liquid coacervates. Reprinted with permission from ref. 100. Copyright 2015 Wiley-VCH Verlag GmbH & Co. KGaA.
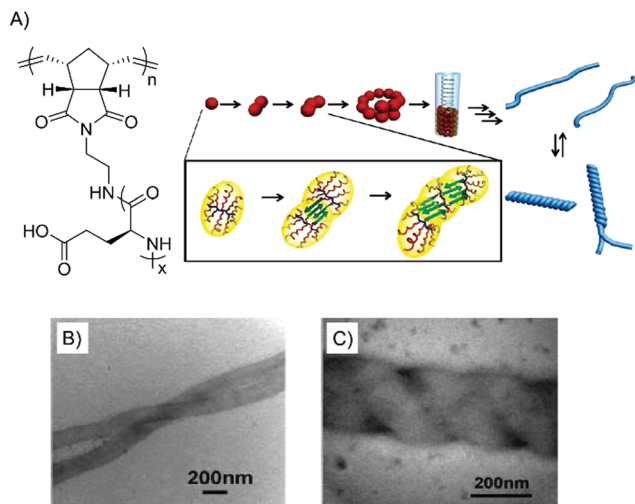
This journal is © The Royal Society of Chemistry 2018

Chem. Soc. Rev., 2018, 47, 7401–7425 | 7409

Fig. 9 Topology induced anti-parallel β-sheets. (A) Schematic illustration of PN-*g*-PLG forming tubular superstructures. The interactions between PLG chains from brush-like PN-*g*-PLG polymers result in the formation of anti-parallel β-sheets, which further induces helical tubular super-structures. (B and C) TEM images of the helical tubular structures from PN_{11}-*g*-PLG_{101}. Scale bar = 200 nm. Reprinted with permission from ref. 121. Copyright 2011 American Chemical Society.
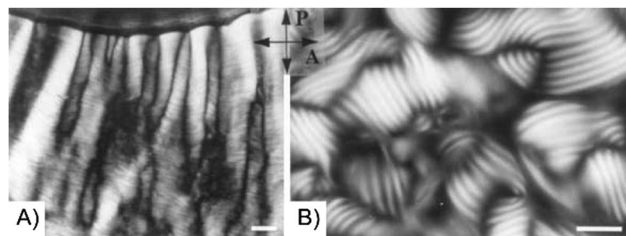

Fig. 10 Formation of LCs from α-helical polypeptides. Pre-cholesteric band texture (A) and cholesteric fingerprints (B) of collagen as viewed by polarized light microscopy between an analyzer (A) and a polarizer (P) which are crossed. Scale bar = 10 μm. Reprinted with permission from ref. 129. Copyright 2003 Elsevier.

the polymers, PLG chains from different molecules aligned with each other and formed anti-parallel β-sheets (Fig. 9A). Consequently, helical tubular structures were induced, as revealed by transmission electron microscopy (TEM) images (Fig. 9B and C). The general applicability of these comb-like structures in inducing the formation of anti-parallel β-sheets and eventually the helical tubular structures was also demonstrated with PLG-grafted Au nanoparticles (NPs).[121,122]

3.5 Liquid crystalline structures from α-helical polypeptides

Certain polypeptides which exhibit an α-helical structure have been demonstrated to form cholesteric liquid crystals (LCs) in solution. This can be linked to and explained by Flory's theories on the necessary criteria for a macromolecular system to nucleate a LC phase: their exhibiting a "rigid, rod-like" structure and being dissolved in a sufficiently high concentration in solution.[123] The first polypeptide-based LC was discovered by Elliot and Ambrose in 1950, when they discovered a birefringent phase present in a chloroform solution of PBLG.[124] However, it was not until a few years later that Robinson utilized the same system to show that these polypeptides organized themselves into LCs of cholesteric nature.[125] Robinson also demonstrated that the transition from a uniform, isotropic phase to a continuous birefringent phase included an intermediate region where there was a coexistence of both phases. It was further noted that the point at which there was the inception of the birefringent phase, and the complete conversion of the isotropic-to-anisotropic phase, was heavily dependent on the MW but not the system solvent; in line with Flory's theory.

The formation of LCs has been identified for homochiral polypeptides regardless of their handedness (*e.g.*, PBLG and poly(γ-benzyl-D-glutamate) (PBDG)).[126] The α-helical conformation

of the polypeptide chain is what provides it with a "rigid, rod-like" characteristic, which is required for the formation of LCs. Equimolar mixing of PBLG and PBDG has been shown to form nematic LCs instead of cholesteric ones, a phenomenon that has been previously observed for binary mixtures of other cholesteric LCs.[126] Phase diagrams produced from experimental data have been shown to behave as Flory's theories predict.[127] For polypeptide LCs, they are most commonly functions of temperature and polypeptide concentration. Interestingly, studies where the nucleation of LC phases was of interest have shown that the initial LC phase nucleates as spherulites, similar to a semi-crystalline polymer nucleating its crystalline phase upon reaching its melting temperature (Fig. 10A and B).[128,129] Furthermore, it was found that the underlying kinetics behind the nucleation of these LC spherulites very intimately matched those of a regular polymer undergoing classical crystallization, proving that the analogy of the LC phase being 'nucleated' is an appropriate one.

4 *In situ* regulation of self-assembly by controlling secondary structures

In linear polypeptides, their ability to instantly form self-assemblies often implies a poor solubility or dispersity in water. This requires special processing procedures to facilitate an even mixture and a well-ordered self-assembly, which typically include its treatment with organic solvents,[70] sonication,[91] or high temperature processing.[130] In nature, globular proteins,[131] which typically form helical and tubular filaments under mild conditions, overcome this problem by starting in conformations that do not easily assemble into higher ordered structures.[131,132] Such proteins are typically highly soluble and monodisperse. Upon exposure to a particular triggering factor (*e.g.*, the binding with adenosine triphosphate (ATP) or guanosine-5′-triphosphate (GTP)), the secondary structures of these proteins are altered, which eventually leads to a cooperative self-assembly.[119,133] On the other hand, disassembly may also be readily achievable with an opposite trigger (*e.g.*, the conversion from ATP bound proteins to adenosine diphosphate (ADP) bound proteins) that induces changes in the secondary structures.[134,135] Inspired by these processes, *in situ* triggered assembly or disassembly has

7410 | *Chem. Soc. Rev.*, 2018, 47, 7401–7425

This journal is © The Royal Society of Chemistry 2018

been realized in synthetic polypeptide systems by controlling the secondary structures *via* enzymatic or chemically coupled modification of side chains or changes in environmental factors.

4.1 Regulation by enzyme triggered reactions

Being highly efficient and selective in catalyzing a large variety of substrates under mild conditions, enzymes are often selected as stimuli to elicit highly specific chemical responses in a system.[136] The most popular enzymatic reactions include phosphorylation/dephosphorylation,[122,137–140] ester hydrolysis,[141,142] amide bond cleavage, reverse hydrolysis,[143] and reduction/oxidation reactions.[144] These reactions have been used to change the hydrophilicity/hydrophobicity or the linkage of the precursors, and consequently induce their assembly or disassembly.[145]

Enzymatic reactions were also used in the polypeptide system to trigger reactions which can induce changes in the secondary structures and hence their self-assembly behaviors. Deming and co-workers demonstrated that *via* an enzyme catalyzed redox reaction, the hydrophilic, disordered polypeptide, poly(L-methionine sulfoxide) (PLMetO), can be reduced to hydrophobic, α-helical poly(L-methionine) (PLMet) (Fig. 11A).[93]
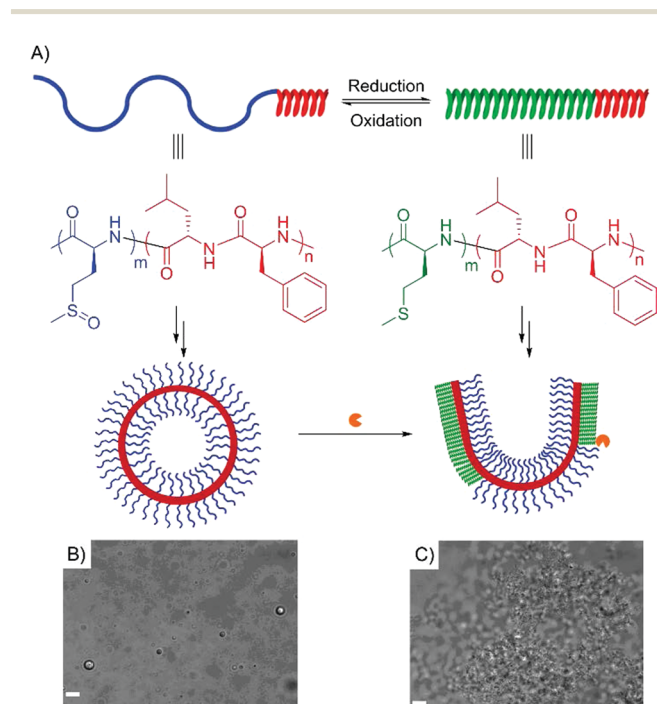

Fig. 11 Enzyme-catalyzed disassembly of copolypeptide vesicles. (A) Scheme showing the rupture of PLMetO$_{65}$-*b*-(PLLeu$_{10}$-*r*-PLPhe$_{10}$) vesicles upon reduction under the catalysis of methionine sulfoxide reductases A and B. The reduction of methionine sulfoxide to methionine alters the secondary structure of the hydrophilic block, resulting in the disruption of the vesicular morphology. (B and C) Differential interference contrast (DIC) images of vesicle suspensions (B) and vesicles incubated with DTT and methionine sulfoxide reductases A and B at 37 °C for 16 h (C). After the treatment with the reductant and enzyme, the spherical vesicular morphology (B) changes to precipitates with irregular sheet-like structures (C). Scale bar = 5 μm. Reprinted with permission from ref. 93. Copyright 2013 American Chemical Society.

A diblock amphiphilic copolypeptide with hydrophilic PLMetO and hydrophobic, α-helical PLLeu-*r*-poly(L-phenylalanine) (PLPhe) is able to self-assemble into vesicles in aqueous solution (Fig. 11B). When methionine sulfoxide reductases A and B were added, the PLMetO was reduced to PLMet, making the diblock polypeptide a completely α-helical, hydrophobic rod (Fig. 11A). As a result, the vesicles were disrupted, and irregular sheet-like structures were observed from differential interference contrast (DIC) images (Fig. 11C).

4.2 Regulation by chemical modification

Another method for *in situ* manipulation of the secondary structure is by chemical modification of the side chain structures of polypeptides. For instance, modifications can be achieved through UV irradiation or the addition of chemical reactants.

Cheng, Leal, and co-workers reported the development of a polymersome based on a PEG-*b*-PDMNBLG, which undergoes a helix-to-coil transition under UV irradiation.[70] The UV triggered cleavage of side-chain ester bonds on the PDMNBLG block not only led to the loss of the α-helical conformation of the polypeptide block, but also rendered the entire block copolymer hydrophilic, causing a disassembly of the polymersomes.

The manipulation of secondary structures has also been performed through the addition of chemicals and catalysts to induce *in situ* reactions. Lin, Cheng, and co-workers have shown a coil-to-helix transition by modifying PLG-grafted comb copolymers with benzylamine in the presence of a coupling catalyst (Fig. 12A).[146] The stacking of side-chain benzyl rings enhanced the side-by-side interactions of α-helices through hydrophobic interactions (Fig. 12B), resulting in the assembly of comb copolymers into membranes (Fig. 12C and D).

4.3 Regulation by pH or salts

Polypeptides bearing side-chain amines or carboxylic acids are sensitive to solution pH and ionic strength. Side-chain charge interactions disrupt the formation of α-helices and β-sheets due to intra- or inter-chain repulsions, while salt can be used to partially or completely screen these charge interactions depending on its concentrations.[91,147]

Lecommandoux and Rodriguez-Hernandez demonstrated a "schizophrenic" polypeptide-based polymersome in which the hydrophilic and hydrophobic segments are entirely dependent on the pH of the assembly medium (Fig. 13A).[148] The diblock copolypeptide, PLG-*b*-PLL, exhibited a random coil structure between pH 5 and 9 since both blocks were in their charged states. At pHs below 4, the protonation of the PLG block led to its coil-to-helix transition, resulting in the assembly of vesicles, with helical PLG forming the interlayer and the charged PLL forming the corona (Fig. 13B). At elevated pHs, the roles of the blocks were reversed, resulting in polymersomes with a neutral PLL interlayer and a negatively charged PLG surface (Fig. 13C).

Reports of salts being utilized to screen intramolecular charge repulsion and stabilize the α-helices have been around for several decades.[149] Multiple studies have since been conducted to demonstrate the influence of ionic strength on the

This journal is © The Royal Society of Chemistry 2018

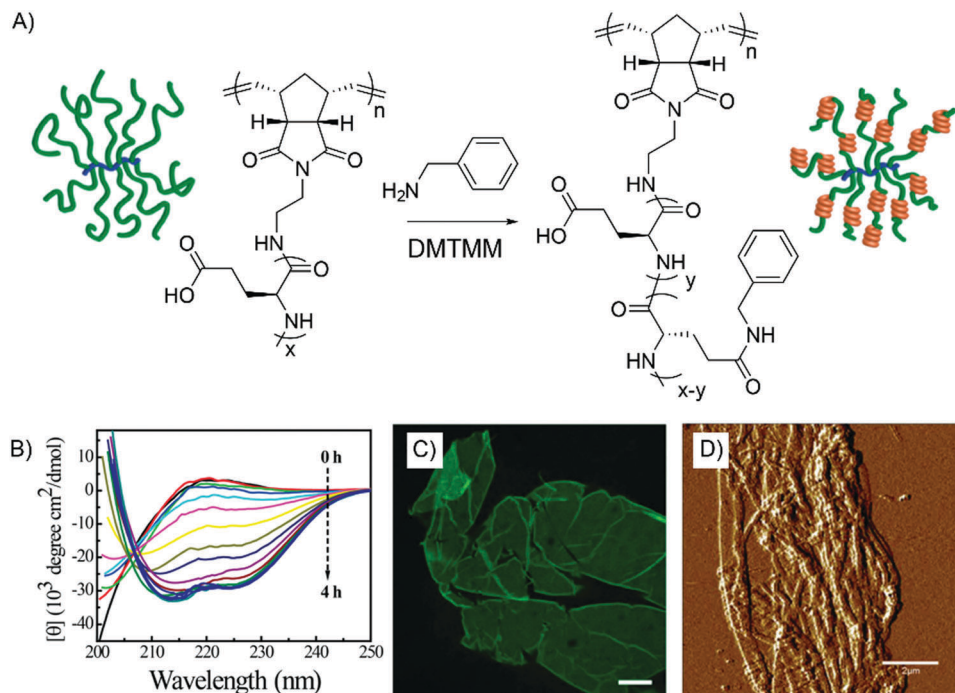*Chem. Soc. Rev.*, 2018, **47**, 7401–7425 | **7411**

Fig. 12 Chemical modification induced self-assembly of polypeptide-based copolymers. (A) Scheme showing the modification of PN-*g*-PLG by benzylamine and the accompanying secondary structure change from random coils to α-helices. 4-(4,6-Dimethoxy-1,3,5-triazin-2-yl)-4-methyl morpholinium chloride (DMTMM) is used as the coupling agent. (B) CD spectra revealing the time progress of the conformational changes in PLGs after PN_{10}-*g*-PLG_{102} reacts with benzylamine (0.5 mg mL^{-1} polymer, pH = 7, rt). The amidation reaction converts charged PLG residues into neutral residues, leading to coil-to-helix transitions. (C and D) Confocal microscopy (C, stained with Thioflavin T) and AFM amplitude (D) images of thin membranes assembled from benzylamine substituted PN_{10}-*g*-PLG_{102} samples. Scale bar = 20 μm for (C) and 2 μm for (D). Reprinted with permission from ref. 146. Copyright 2017 American Chemical Society.

secondary structure of polypeptides, leading to the assembly into complex architectures with useful properties. Pochan and co-workers reported a salt-triggered self-assembly of polypeptides into hydrogels based on β-hairpin peptides.[150] The increase of the ionic strength weakened the interactions between charged side chains, facilitating the folding of polypeptides into β-sheets. Upon further increase in salt concentration, continually enhanced mechanical properties of the hydrogel (*e.g.*, storage modulus) were observed.

4.4 Induced secondary structure by metal coordination

The coordination of metal ions with charged polypeptides is another way to neutralize charges and further trigger the self-assembly through the coil-to-helix transition. For instance, Kataoka and co-workers reported the use of a PEG-*b*-PLG derivative for the preparation of polymersomes *via* metal coordination.[151] The binding between (1,2-diaminocyclohexane)-platinum(II) (DACHPt) and the negatively charged PLG block decreases the electrostatic repulsions, leading to the spontaneous formation of metallosomes (Fig. 14A). The coil-to-helix transition of the PLG block was confirmed by CD spectra of the copolymers before and after the addition of DCHPt (Fig. 14B). Interestingly, although the release of DACHPt under physiological conditions caused a gradual decrease of the CD signal, the characteristic CD spectra of the α-helix remained even after a prolonged incubation time of 124 h (Fig. 14C). The α-helical

structures played an important role in maintaining the vesicular morphology of metallosomes, and hence retaining the encapsulated cargos. The vesicular structures were still visible after 48 h incubation of metallosomes under physiological conditions, even with >40% loss of DACHPt.

5 Formation of amyloid fibrils by synthetic polypeptides

Amyloid fibrils are starch-like proteinaceous fibrils which are characterized by a cross-β structure. They have been associated with more than 20 human diseases, including Alzheimer's disease, Huntington's disease, and type II diabetes.[152,153] At the same time, amyloid fibrils possess excellent mechanical properties that are comparable to natural building blocks (*e.g.*, microtubules and actin filaments), which makes them promising materials for biomedical applications.[154] In this section, we focus on the amyloidogenic behavior of synthetic polypeptides and their potential applications as functional materials.

5.1 Amyloidogenesis is exhibited by widely different polypeptides

The formation of amyloid fibrils has been associated with specific sequences and compositions of amyloidogenic proteins.[155–157] In 2002, Fändrich and Dobson induced the formation of amyloid
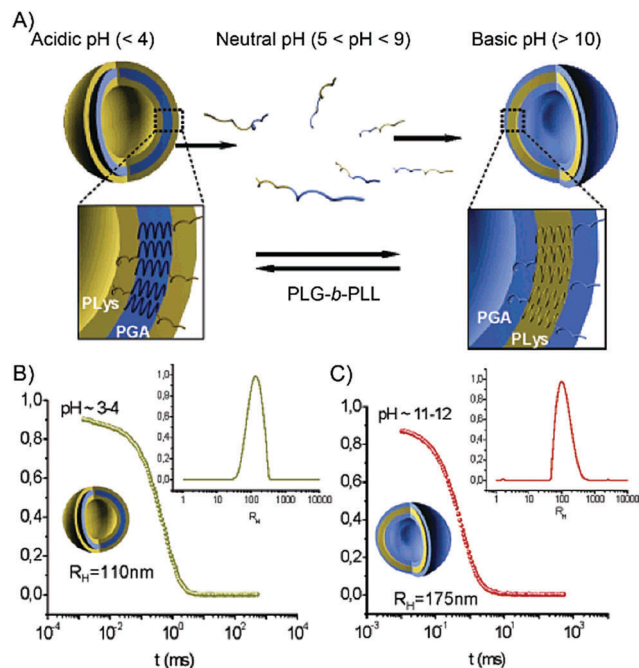
Fig. 13 pH-Responsive, reversible assembly and disassembly of copoly-peptides. (A) Scheme showing the pH-responsive self-assembly of PLG-b-PLL into a vesicular morphology. At pH < 4, the PLG segment forms a neutral α-helical structure and remains in the interlayer, while the charged PLL block adopts a random coil conformation and remains in the corona. The interlayer and corona are reversed at pH > 10. (B and C) Auto correlation functions (90°) of PLG_{15}-b-PLL_{15} at pH = 3 (B) and pH = 12 (C). The corresponding R_H distributions are shown in the insets. Reprinted with permission from ref. 148. Copyright 2005 American Chemical Society.
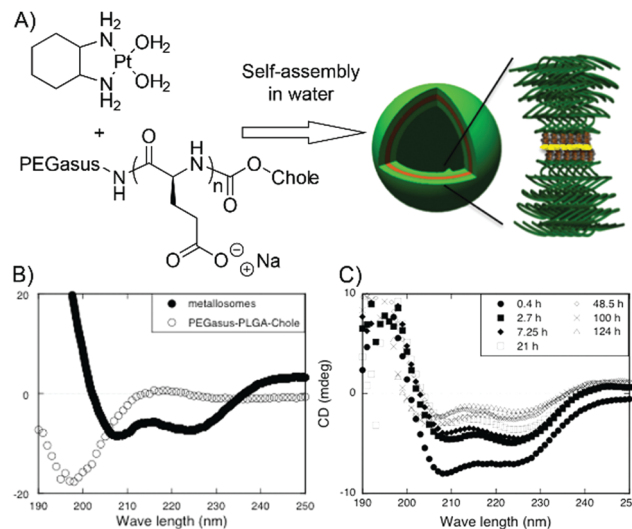

Fig. 14 Formation of metallosomes induced by the metal coordination of polypeptide-based copolymers. (A) Scheme illustrating the formation of metallosomes through the metal coordination induced coil-to-helix transition. (B) CD spectra of PEG-b-PLG derivatives in solution and upon addition of a Pt complex. The coordination between the Pt complex and the PLG residue reduces intra-chain charge repulsions, resulting in the formation of α-helices. (C) CD spectra of metallosomes incubated under physiological conditions for different lengths of time. During the incuba-tion, the gradual release of the Pt complex leads to a decrease of helicity in the metallosome. However, the helical conformation is retained even after 124 h incubation. Reprinted with permission from ref. 151. Copyright 2012 American Chemical Society.

fibrils at high temperature using various polypeptides bearing different side chains,[158] including PLL (Fig. 15A), PLG (Fig. 15B), and poly(L-threonine) (PLThr) (Fig. 15C). They demonstrated that the formation of amyloid fibrils is dictated by main chain inter-actions, which is a generic property among all polypeptides and requires no specific sequence. The sequence and side chain interactions of polypeptides, including hydrophobic and charge interactions,[158–160] influence the morphology of the aggregates and the kinetics and solution conditions of fibril formation. In addition, Huang and co-workers further confirmed the determin-ing role of amide backbones by showing the formation of amyloid fibrils with random copolypeptides[160] and poly(ε-L-lysine) (ε-PL).[161]

The generality of the amyloidogenic properties of poly-peptides comes from the fact that neutral β-sheets are thermo-dynamically more favorable than α-helices and random coils, even though α-helices are kinetically more favorable than β-sheets (Fig. 15D). Thus, the α-helix must first be destabilized in order to achieve β-sheet structures. For instance, Cieślik-Boczula reported that when low-temperature alkaline solutions or methanol-rich water solutions were used, the formation of α-helical fibrils of PLL with unordered and gauche-rich hydro-carbon side chains was observed.[162] The formation of antiparallel β-sheet-rich fibrils with highly ordered trans-rich hydrocarbon side chains, on the other hand, was only observed with high-temperature alkaline solutions where the α-helices were destabilized.

5.2 The influence of chirality

The chirality of polypeptides plays an important role in influ-encing the formation of amyloid fibrils. Dzwolak and co-workers found that the chirality influenced the secondary structures and superstructures of polypeptides.[163–165] They have shown that when enantiomerically pure PLGs or poly-(D-glutamic acid)s (PDGs) were incubated, spirally twisted superstructures were obtained. These spirally twisted super-structures were found to contain $β_2$ fibrils with an amide I band peak at 1595 cm^{-1}, which was attributed to the networks of bifurcated H-bonds coupling C=O and N–H groups of the main chains and side chains. When a mixture of PLGs and PDGs was used to grow fibrils, no ordered structures were detected by scanning electron microscopy (SEM). The aggre-gates were found to be composed of $β_1$ fibrils with amide I bands at 1684 and 1612 cm^{-1}. Since $β_1$ fibrils are thermodyna-mically less stable than $β_2$ fibrils, they were converted into $β_2$ fibrils at high pressures.[166]

5.3 The influence of chain length

Chain lengths and polydispersity have been demonstrated to play a critical role in controlling the formation rate and morphology of amyloid fibrils. Dzwolak and co-workers reported that n = 4 is the critical DP for PLGs to form amyloid fibrils,[167] and that the morphology of the aggregates varied depending on the chain lengths of PLGs (Fig. 16A and B). Interestingly, despite these differences in morphology, all PLGs
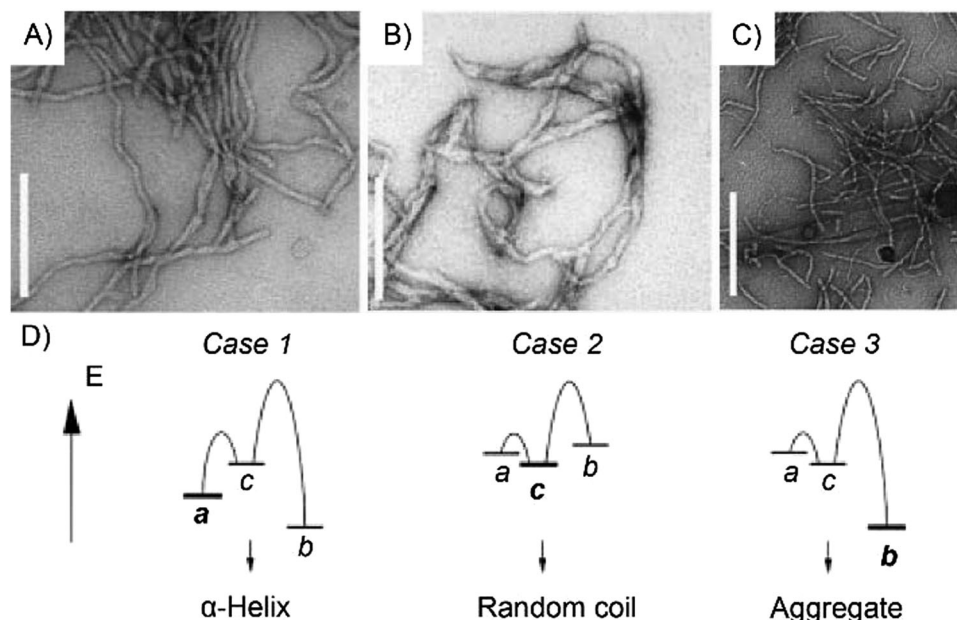
Fig. 15 Amyloidogenesis of polypeptides. (A–C) EM images of amyloid fibrils from various polypeptides. (A) PLL (2.5 mg mL^{-1}, H$_2$O, pH = 11.2, 65 °C, 4 d), (B) PLG (1 mg mL^{-1}, D$_2$O, pD = 4.08, 65 °C, 2 d), and (C) PLThr (10 mg mL^{-1}, H$_2$O, 50 mM sodium borate, pH = 9.0, 65 °C, 4 d). Scale bar = 200 nm. (D) The partitioning between the folding and amyloid formation of PLL. Case 1: In the neutral state, the α-helix (a) is kinetically more favorable than the β-sheet (b). Case 2: In the charged state, the random coil conformation (c) has the lowest energy. Case 3: In the neutral state, the β-sheet is observed under conditions that destabilize the α-helix (e.g., mild heating). Reprinted with permission from ref. 158. Copyright 2002 Wiley-VCH Verlag GmbH & Co. KGaA.

were composed of β$_2$ fibrils and shared a uniform diameter, suggesting a common self-assembly pathway for PLGs with different chain lengths.

Additionally, the chain lengths and chain length polydispersity have also been demonstrated to have an important effect on the kinetics of amyloidogenesis. PLGs with longer chains assembled more rapidly than those with shorter chains.[168] Surprisingly, a mixture of PLG$_5$ and PLG$_{200}$ assembled significantly more rapidly than separate assemblies of the two polypeptides (Fig. 16C), which was attributed to misfolding transfers from PLG$_5$ to PLG$_{200}$.

5.4 Potential applications of polypeptides in amyloid functional materials

With a rich and ordered H-bonding network at their core,[169–171] amyloid fibrils exhibit high cohesive energy and exceptionally large persistent lengths,[172,173] which are independent of their environment. Amyloid fibrils can be used as structural materials due to their rigid, cohesive nature and their high resistance against degradation by chemical or biological processes. In fact, the elastic moduli of amyloid fibrils are comparable to those of collagen, keratin, and silk.[154] The properties of these fibrils were exploited in biofilms of many bacteria including *Escherichia coli*,[174] the eggshells of silkmoths,[175] and natural adhesives used by algae.[176] Besides these natural findings, amyloid fibrils are also used in applications such as long-term drug release,[177] the formation of nanocomposites,[178,179] gel scaffolds,[180] biosensors,[181,182] the amyloid-mediated synthesis of hybrid organic/inorganic materials,[183–185] and amyloid-templated optoelectronic materials.[186–191]
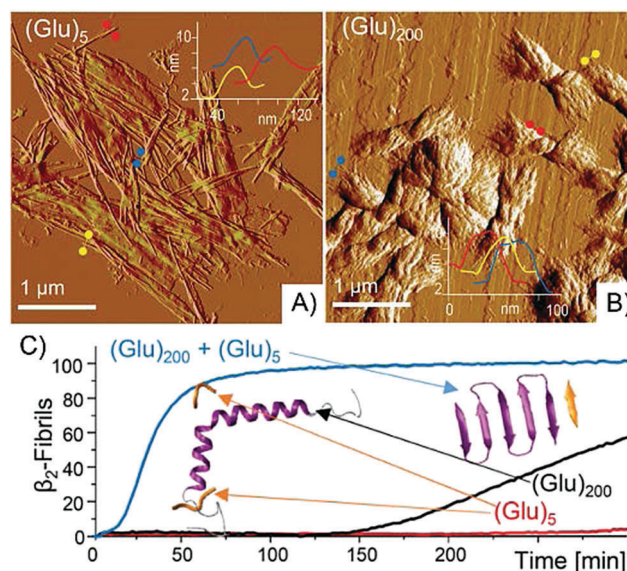

Fig. 16 The influence of chain lengths on the formation of amyloid fibrils. (A and B) AFM tapping-mode images of PLG$_5$ (A) and PLG$_{200}$ (B). Scale bar = 1 μm. The cross sections of selected fibrillary specimens are shown in the insets. The thickness of the fibril is independent of the chain length of PLG. Both samples are longer than the critical length to form amyloid fibrils. As a result, long, straight, and unbranched fibrils are observed in both images. Reprinted with permission from ref. 167. Copyright 2015 American Chemical Society. (C) Fibrilization kinetics of PLG$_5$ and PLG$_{200}$, and their mixtures at 40 °C. By mixing the short PLG with the long PLG, the fibrillization rate is greatly enhanced. Reprinted with permission from ref. 168. Copyright 2016 American Chemical Society.

Though amyloid fibrils have found many applications, most of them are still made of proteins or peptides. Considering that

7414 | *Chem. Soc. Rev.*, 2018, **47**, 7401–7425

This journal is © The Royal Society of Chemistry 2018

all polypeptides have a general propensity to form amyloid fibrils, synthetic polypeptides have great potential in the applications of amyloid-based materials.

6 Secondary structure associated biomedical performance of polypeptides

Synthetic polypeptides provide a promising platform of materials for biomedical applications due to their great biocompatibility and biodegradability. There are numerous reports which utilize polypeptide-based materials in areas such as drug delivery, gene delivery, antimicrobial peptides, and tissue engineering. Many reviews have focused on summarizing progress of polypeptide materials in these applications.[23,28–33] In this section, we will mainly discuss the conformation-specific performances of synthetic polypeptides.

6.1 Impact of secondary structures on drug delivery applications

Polypeptide materials have been reported to serve as a class of promising polymeric drug carriers for the delivery of both therapeutic small molecules and macromolecules to disease sites.[30,192–194] Polypeptides adopting different secondary structures exhibit different co-assembly behaviors with encapsulated or conjugated drug molecules, resulting in distinct biomedical performances.

Kataoka and co-workers reported the effects of bundled α-helices on the assembly behaviors of *cis*-dichlorodiammine-platinum(II) (cisplatin, CDDP)-loaded polymeric micelles (CDDP/m).[107] In this work, the authors compared CDDP/m formulated from polypeptides with identical chemical backbones but different chiralities. The L-CDDP/m and D-CDDP/m, which were assembled from cisplatin with PLG and PDG, respectively, showed a higher micelle yield as compared to DL-CDDP/m formulated from cisplatin with poly(DL-glutamic acid)s (PDLGs). The improved yield was attributed to increased hydrophobicity as the driving force for the assembly, which was provided by the lateral alignment of α-helical polypeptides in the core of the CDDP/m (Fig. 17A). The formation of α-helices also significantly affected cisplatin release under physiological conditions, in which a slower release profile of cisplatin was achieved in L-CDDP/m and D-CDDP/m as compared to DL-CDDP/m. Based on the analysis of the release profiles of polymer dimers and unimers, the authors concluded that the densely packed micelle core of L-CDDP/m and D-CDDP/m prevented the penetration of water molecules and chloride ions, thus displaying a prolonged release profile that resulted from an "erosion-like process" of micelle disassembly (Fig. 17B). In contrast, the accelerated release of cisplatin from DL-CDDP/m can be explained by the synergistic effect of disassembly from the loss of hydrophobicity and the penetration of water molecules and chloride ions into the micelle core (Fig. 17B). These distinctly different drug releasing profiles resulted in different biodistributions of cisplatin in mouse organs. L-CDDP/m and D-CDDP/m, with a

bundled helix core, exhibited prolonged circulation in plasma (Fig. 17C), decreased accumulation in the liver and spleen, enhanced tumor accumulation (Fig. 17D), and anti-tumor efficacy as compared to DL-CDDP/m. This work demonstrates the significant role of polypeptide secondary structures in drug delivery outcome under complex physiological conditions.

As previously mentioned, drug molecules are commonly chemically conjugated on polypeptide side chains or physically encapsulated in polypeptide-based assembly. In some cases, the ordered secondary structures of polypeptides hinder the co-assembly/encapsulation of drugs because of their strong tendency to self-assemble. Semple and co-workers recently reported that the chirality of the polypeptide influenced the drug loading into polypeptide micelles.[195] Micelles formulated with PEG-*b*-poly(γ-benzyl-DL-glutamate) (PBDLG) amphiphiles showed increased irinotecan loading compared with those formulated with PEG-*b*-PBLG. The authors attributed the enhanced drug loading efficiency not only to the increase of the overall flexibility of random coil structures over their α-helical analogues, but also to the preference of PBDLG blocks to co-assemble with drug molecules rather than packing into α-helical bundles.

6.2 Impact of secondary structures on gene delivery applications

Cationic polymers are able to form nanocomplexes with DNA or RNA molecules through electrostatic interactions.[196] These nanocomplexes showed different levels of efficiency in the delivery of nucleic acids into mammalian cells and the final gene expression outcome. The secondary structure of polypeptide materials offers an extra parameter to manipulate the performance and efficiency of gene delivery.

The nanocomplexes of polypeptides and nucleic acids are typically internalized through endocytosis in mammalian cells. In order to achieve high efficiency of gene delivery, the nucleic acids have to escape from endosomes and enter the cytoplasm or nucleus. Apart from utilizing the proton sponge effects with side-chain amines,[196] the secondary structure of polypeptide materials provides a unique solution to tackle these challenges. Cheng, Wang, and co-workers reported the use of cationic, α-helical polypeptide materials for efficient delivery of model plasmids into mammalian cells.[62] From a polypeptide library with 31 different amine side chains, the best polypeptide, poly(γ-4-((2-(piperidin-1-yl)ethyl)aminomethyl)benzyl-L-glutamate) (PPABLG, also named PVBLG-8), displayed the highest transfection efficiency in COS-7 cells as assayed by Luciferase expression, outperforming conventional transfection agents such as polyethylenimine (PEI) and PLL. Unlike PLL, which adopts the random coil conformation under physiological conditions and lacks any endosomal escape capability, α-helical PPABLG showed enhanced endosomal escape through endosomal membrane disruption. The membrane disruption capability was significantly reduced when the secondary structure was removed from the polypeptide. The racemic analogue, PPABDLG, exhibited much lower transfection efficiency than PPABLG, demonstrating the essential role of secondary structures in achieving high gene delivery efficiency.
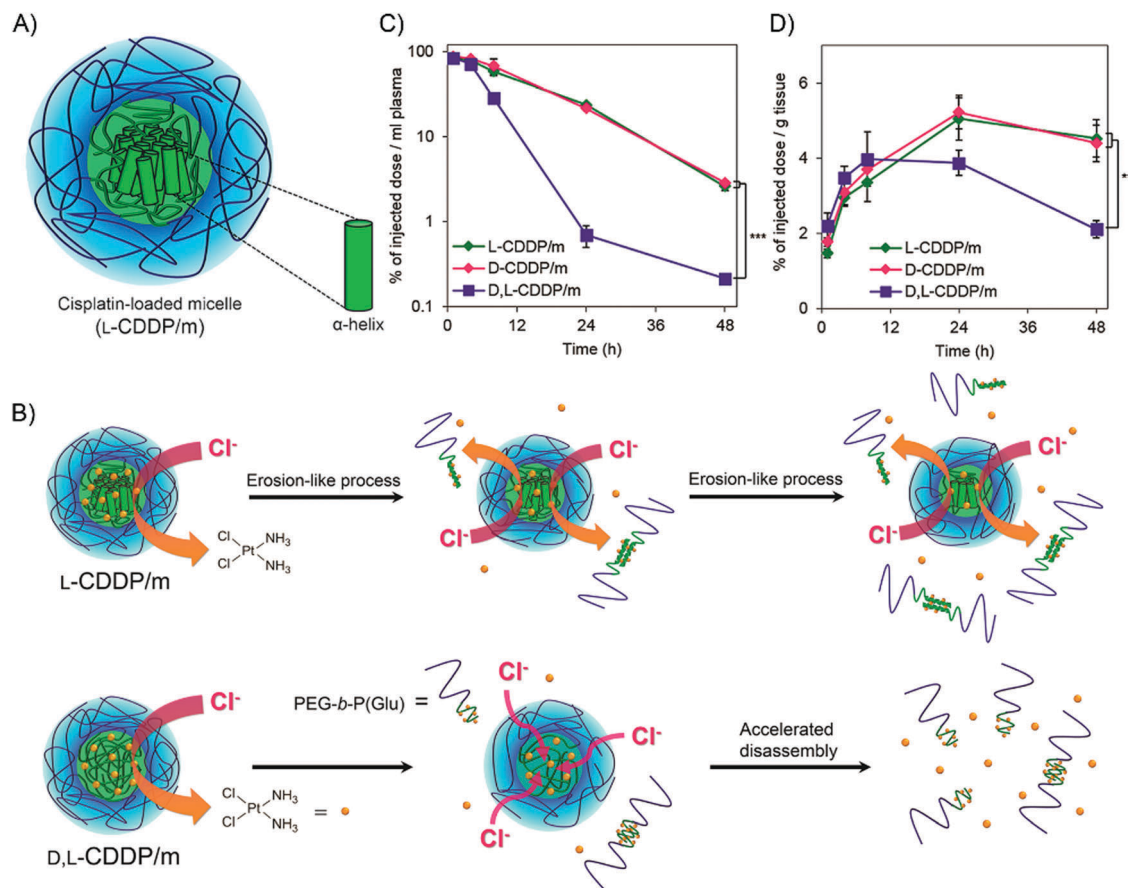
This journal is © The Royal Society of Chemistry 2018

Chem. Soc. Rev., 2018, 47, 7401–7425 | 7415

Fig. 17 Structure−property correlation in a polypeptide-based micellar drug delivery system. (A) Scheme illustrating the formation of CDDP/m micelles. The lateral alignment of α-helices facilitates the self-assembly process, resulting in an improved yield of micelles. (B) Schematic illustrations of drug release mechanisms from L-CDDP/m and D,L-CDDP/m. In the top figure illustrating the drug release from L-CDDP/m, the close packing of α-helices prevents the penetration of water and Cl⁻, leading to an erosion-like process with delayed drug release. In contrast, D,L-CDDP/m, without ordered secondary structures, exhibits accelerated drug release. (C and D) Pharmacokinetics of a platinum drug (C) and biodistribution in tumor tissues (D) with L-CDDP/m, D-CDDP/m, and D,L-CDDP/m. Prolonged circulation in plasma (C) and enhanced tumor accumulation (D) are observed for L-CDDP/m and D-CDDP/m with helical polypeptide building blocks. Reprinted with permission from ref. 107. Copyright 2014 American Chemical Society.

Apart from PPABLG,[41,197–206] secondary structure-associated membrane activity was also demonstrated in other synthetic polypeptides with cationic side chains such as primary amines,[64] guanidines,[41,64,207] quaternary ammoniums,[53] and quaternary phosphoniums.[63] The membrane activities of these α-helical polypeptides prepared from chiral NCA monomers are significantly higher than their analogs synthesized from racemic NCA monomers with identical chemical structures.

Apart from secondary structures and side-chain cationic groups, the chain lengths of polypeptides also play an important role in gene delivery applications, influencing both membrane activity and nucleic acid condensation. Cheng and co-workers reported helical poly(arginine) mimics with backbone length dependent cell-penetrating properties.[207] In particular, a helical polypeptide with DP = 72 showed three times higher cell penetration than its shorter analog with only 10 repeating units. Cationic polypeptides with longer chain lengths also displayed higher pore formation capability. For efficient condensation of negatively charged nucleic acids, the length of cationic polypeptides needs to exceed a certain threshold. Multiple reports have shown that short polypeptides such as CPP (10–25 peptide residues) are not able to form stable nanocomplexes with DNA or siRNA.[41,62]

Moreover, the interactions between cationic, α-helical polypeptides and anionic lipid membranes have been investigated in detail to elucidate the role of secondary structures.[208] From molecular dynamics simulations of interactions between cationic polypeptides and negatively charged lipid bilayers, it was revealed that the rigid α-helical polypeptide core and quasi-liquid polypeptide surface enabled adaptable "landing", "anchoring", and "tunneling" of polypeptides onto lipids (Fig. 18A–D). As a result, the insertion of α-helical polypeptide restructured lipid vesicles into phases rich in negative Gaussian curvature (NGC), as characterized by small-angle X-ray scattering (SAXS). The formation of the NGC agreed with the experimental observations of pore formation and membrane permeation/destabilization. On the other hand, random-coil polypeptides from racemic monomers were not able to generate NGC and showed significantly lower membrane permeability from both simulation and experimental results.
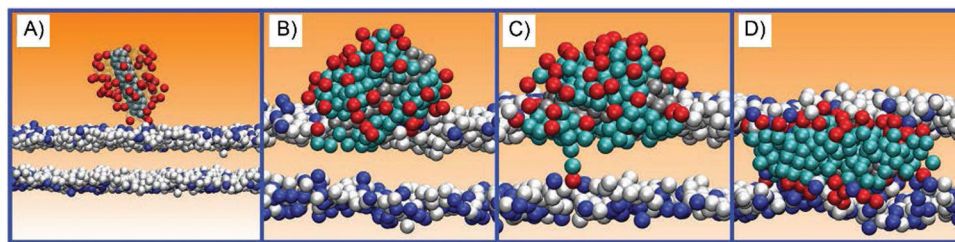
7416 | Chem. Soc. Rev., 2018, 47, 7401–7425

This journal is © The Royal Society of Chemistry 2018

Fig. 18 The interaction of helical, cationic polypeptides with a membrane. Sequences of simulation images are presented illustrating the landing (A), initial anchoring (B), initial tunneling (C), and full insertion in a membrane–spanning state (D). The rigid helical core and the mobile side chains plays important roles in the insertion process. The polypeptide has 4-bead long side chains, of which 100% have charged termini. The hydrophobic components of the side chains are colored in cyan, and the peptide core is depicted in gray. The remaining beads are color coded based on their charges: red for +1e, white for uncharged, and blue for −1e. Reprinted with permission from ref. 208. Copyright 2017 American Chemical Society.

6.3 Impact of secondary structures on antimicrobial applications

Antimicrobial peptides (AMPs) are well-known as sequence controlled, bacteria-killing materials which are naturally produced as part of an innate immune response.[209–212] These AMPs mediate physical disruption of bacterial cell membranes, which is a killing mechanism less likely to develop resistances as compared to small molecule antibiotics.[213] At the same time, AMPs also suffer from stability and toxicity issues,[214,215] which hinder the development of AMPs as therapeutics. Synthetic antimicrobial polypeptides, as one of the most promising analogue systems of native AMPs, have been developed to address these obstacles.

Recently, Cheng and co-workers developed a series of α-helical, radially amphiphilic polypeptides with high antimicrobial activity against both Gram-positive and Gram-negative bacteria.[65] In this work, the secondary structures of synthetic polypeptides played an important role in maximizing their bacteria-killing ability as well as enhancing their selectivity between bacterial and mammalian cells. Radially displayed cationic groups bind efficiently with negatively charged bacterial membranes through charge interaction (Fig. 19A). The rigid, α-helical polypeptide core, in combination with flexible side chains, provided antimicrobial activity through membrane disruption, which was characterized by both SAXS of the lipid model system and SEM observations. Benzimidazole

functionalized poly(γ-(6-chlorohexyl)-ʟ-glutamate) (PHLG-BIm, Fig. 19B) with an α-helical conformation showed a 4–16 times lower minimum inhibitory concentration (MIC) value than its random coiled analogue, PHDLG-BIm, in multiple bacterial strains. The radial structure also decreased the nonspecific interactions between the hydrophobic segments of the polypeptides and eukaryotic cell membranes, resulting in increased selectivity (defined as the ratio of HC50 to MIC). For example, random coiled PHDLG-BIm only showed a selectivity > 2 against DH5α bacteria, while α-helical PHLG-Blm exhibited a selectivity > 32, suggesting the superior selectivity of α-helical polypeptide materials as synthetic AMP analogues. When incorporated with stimuli-responsive moieties, these radially amphiphilic polypeptides were further used as bacteria-sensitive antimicrobial polypeptides[69] and polypeptides for the treatment of *Helicobacter pylori*.[42]

7 Secondary structures in catalysis

One important role of proteins is to catalyze various biochemical reactions in living organisms. In the presence of enzymatic catalysis, many reactions that require harsh conditions to completely become compatible within a mild cellular environment. Inspired by the unique role of enzymes in biological systems, polypeptide scientists have devoted their efforts towards developing "synthetic enzymes". The intrinsic chiral environment provided by stable secondary structures makes synthetic polypeptides good candidates for enantioselective catalysts. Among all the organic asymmetric reactions evaluated, the Juliá–Colonna epoxidation is most studied due to its high chemical and optical yield.

In this section, we will focus on discussing the role of secondary structures of polypeptide catalysts in the Juliá–Colonna epoxidation. The detailed experimental setup, variation of substrates and oxidants, and applications in total synthesis have already been summarized in several excellent review papers,[216,217] and will not be covered here.

7.1 Introduction of the Juliá–Colonna epoxidation

The synthetic polypeptide catalyzed epoxidation of electron-deficient olefins, such as *trans*-chalcones (Fig. 20A), was first reported by Juliá, Colonna, and co-workers in the 1980s.[218–221]
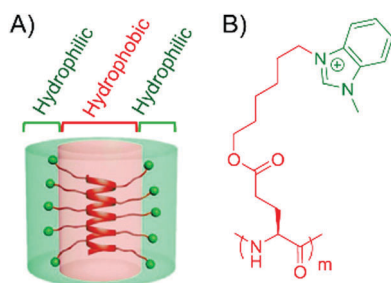

Fig. 19 Scheme illustration (A) and the chemical structure (B) of radially amphiphilic antimicrobial polypeptides, PHLG-BIm. The radial structure facilitates the interactions with bacterial membranes, while reducing non-specific interactions with eukaryotic cell membranes. Reprinted with permission from ref. 65. Copyright 2015 National Academy of Sciences.
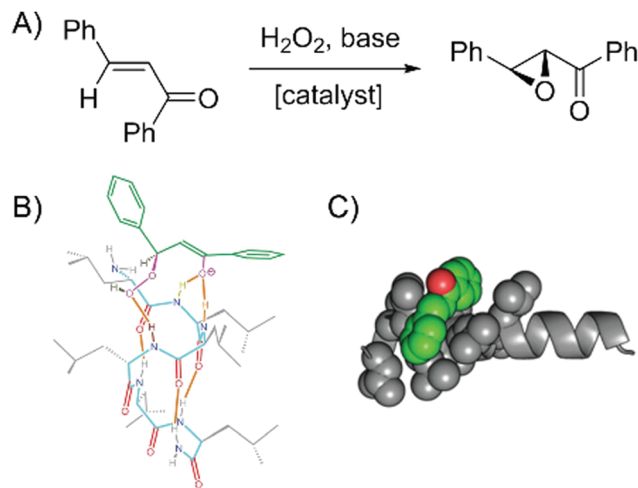
Fig. 20 Juliá–Colonna epoxidation and the proposed reaction mechanism. (A) Synthetic scheme showing the epoxidation of enone in the presence of polypeptide catalysts. (B) The structure of the complex with PLLeu and 3-hydroxyl-chalcone enolate. The enantioselectivity originates from the hydrogen bonding motif as well as the helical conformation of PLLeu. Reprinted with permission from ref. 231. Copyright 2004 Royal Society of Chemistry. (C) Interaction of *trans*-chalcone with PLLeu. PLLeu blocks are presented as grey cartoons and the PLLeu side chains interacting with *trans*-chalcone are presented as spheres. The *trans*-chalcone substrate fits within the hydrophobic, chiral grooves of PLLeu. Reprinted with permission from ref. 224. Copyright 2017 Royal Society of Chemistry.

When PLAla or PLLeu was used as the catalyst, optically active oxiranes were obtained in 96% yield and with 96% enantiomeric excess (e.e.).[219] Following the work of Juliá and Colonna, several research groups have reported the improvement of the asymmetrical epoxidation, including the simplification into biphasic and homogeneous conditions,[222–224] the addition of phase-transfer agents,[225] and the introduction of solid supports.[226] These improvements not only extended the library of substrates, enabling the selective oxidation of enones that were poor substrates in the original triphasic system, but also significantly simplified the reaction and purification procedure.

7.2 The role of secondary structures

In the original reports, Juliá, Colonna, and co-workers demonstrated that the secondary structures of polypeptide catalysts are critical to the asymmetric induction. For instance, replacing α-helical PLAla or PLLeu with synthetic polypeptides that adopted a β-sheet conformation (*e.g.*, PLVal and PLPhe) resulted in not only lower conversion, but also decreased stereoselectivity. Replacing PLAla with poly(D-alanine) (PDAla), on the other hand, led to a similar degree of asymmetric induction but reversed optical rotation, indicating that the stereoselectivity was associated with the helix sense of the polypeptide catalysts. The reaction in the presence of PDLAla showed <10% conversion, further substantiating the importance of the helical conformation in the catalysis. In addition, reactions using PLAla catalysts with DP > 10 showed much better results compared with those using PLAla with DP < 10, which is not sufficient to form stable α-helices. These results collectively

suggested that the α-helical content of the polypeptide catalysts was closely related to the chemical yield and stereoselectivity of the epoxidation. The correlation between the helicity of the polypeptides and the catalytic activity was further confirmed in various helical peptide systems including solid-phase synthesized peptides, PEG-bound peptides, and stapled helical peptides.[227–230]

7.3 Mechanistic studies

Several studies suggested that the N-terminus of a polypeptide played a critical role in catalyzing the epoxidation of the substrate.[223,229] Polypeptides with the N-terminus attached on a solid support, for instance, exhibited no catalytic activity.[229] With experimental supports, it is believed that polypeptide catalysts formed complexes with enone substrates and the hydroperoxide anion oxidant through H-bonding (Fig. 20B). Therefore, the chirality of the α-helix is crucial to control the geometry of the terminal NH groups on polypeptides, which resulted in the enantioselective oxidation of the substrates.[229,231]

Very recently, Voyer and co-workers reported the Juliá–Colonna epoxidation carried out in pure water, where helical polypeptides acted as both catalysts and solubilizing agents.[224] Computational results showed that the substrate fit within the hydrophobic, chiral grooves of the polypeptide (Fig. 20C). The authors proposed a "groove sliding" mechanism in an aqueous environment, where the hydroperoxide anion bound with the N-terminus of the polypeptides, and the substrates slid into the hydrophobic grooves of polypeptides to the N-terminus for the reaction. These mechanistic studies highlighted the importance of the chirality of the polypeptide in catalyzing stereoselective reactions, which contributes to the deep understanding of the structure–property relationship of enzymes.

8 Secondary structures in polymer synthesis

In nature, the growth of polymeric structures often involves the precise three-dimensional assembly of functional elements which enables spatial and temporal control of the polymerization. The polymerization of tubulin and actin, for instance, is governed by nucleators which catalyze the fast growth of these proteins.[232,233] These cooperative interactions, however, were seldom used in the preparation of synthetic polymers due to the difficulties in precisely controlling the assembly of macromolecules.

Although the polymerization kinetics of NCA have been studied since 1950s,[234–236] the mechanisms remain unclear. Recently, Cheng, Lin, and co-workers reported that the formation of α-helical structures in polypeptides is able to catalyze their own growth,[237] highlighting the importance of secondary structures in polymer synthesis. In this section, the observation of proximity-induced rate acceleration and the role of α-helical conformation will be summarized, and the possible mechanism will be discussed.

8.1 Proximity-induced rate acceleration of polypeptide synthesis

When the polymerization of γ-benzyl-L-glutamate NCA (BLG-NCA) was conducted in dichloromethane (DCM), a huge difference in the polymerization rates between linear polymers and brush polymers was observed. In the linear polymerization system with a norbornene-based trimethylsilylamine initiator (NB, Fig. 21A and B), the NCA monomers were slowly consumed, reaching ~30% conversion after 24 h. When NB was pre-polymerized into a macroinitiator (PNB, Fig. 21A and B), however, all BLG-NCA were fully converted within 1 h. By comparing the chemical structures of NB and PNB, the authors attributed the remarkable differences in the polymerization rate to the proximity between initiating sites in linear and brush systems.

The proximity-induced rate acceleration was further confirmed when the PNB macroinitiator was replaced with a random copolymer containing initiating groups (NB) and inert spacers (Ph) (P(NB-r-Ph)). The density of initiating sites decreased with a decrease of the NB content, leading to slower polymerization rates (Fig. 21C). As a comparison, the block copolymer analogues PNB-b-PPh, with the same concentration but closer proximity of initiating groups, exhibited comparable polymerization rates to PNB when used as the macroinitiator (Fig. 21D).

8.2 Secondary structure plays a critical role in cooperative polymerization

With a close examination of the polymerization progress, two-stage kinetics were observed for both the linear and the brush polymerizations, where the rate constant was larger for the second stage. Interestingly, the beginning of the second stage coincided with the formation of α-helices, as evidenced by both CD and FTIR (Fig. 21E), suggesting the critical role of the α-helical conformation in the rate acceleration. In addition, the polymerization of racemic DL monomers resulted in a one-stage, slower polymerization compared with the L and D monomers under similar conditions, since the propagating PBDLG chains adopted a random coil structure. As a comparison, the polymerization of NCA monomers on an existing α-helical PBLG initiator proceeded without the slow first stage, further confirming the helix-associated rate acceleration.

The authors suggested the differences in the macrodipole to be the reason for both the two-stage polymerization kinetics and the substantial rate difference between linear and brush polymerizations (Fig. 21F). The formation of the macrodipole due to the coil-to-helix transition at early polymerization stages greatly enhances the electrostatic environment of the propagating terminus, which is responsible for the increased interaction and polymerization rate of NCA monomers. In the case of brush
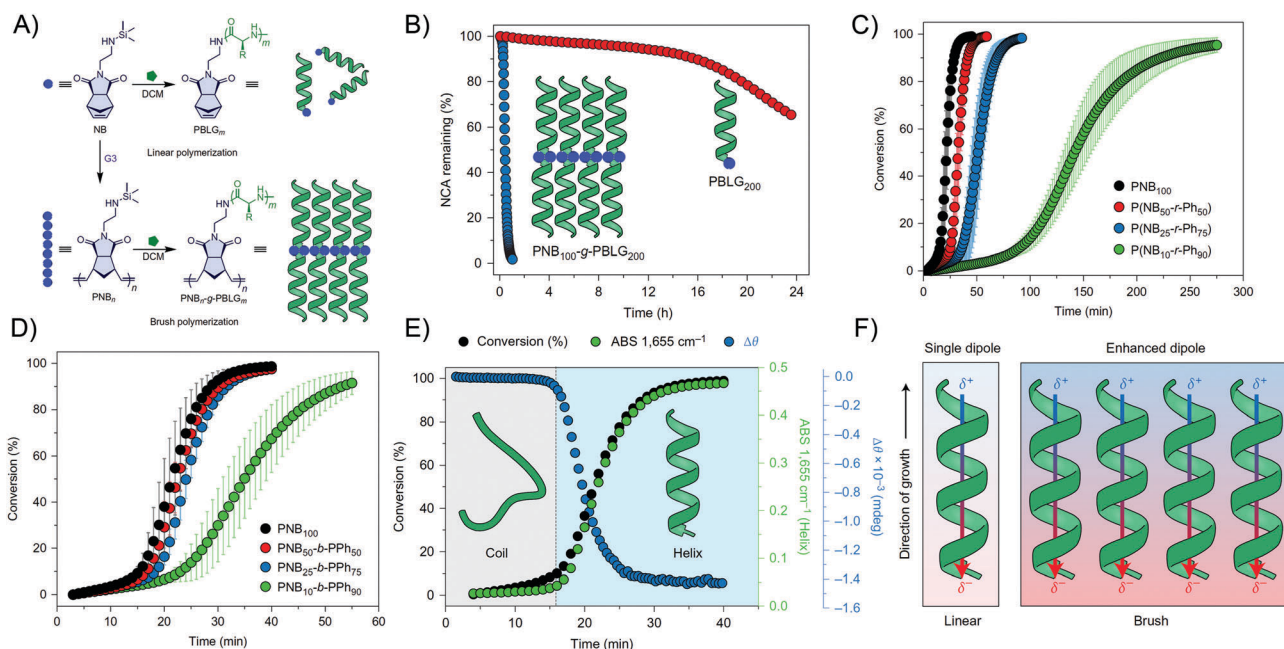

Fig. 21 The role of the α-helical conformation in the proximity-induced acceleration of the polymerization rate. (A) Scheme showing the polymerization from NB initiators (linear) and PNB macroinitiators (brush). (B) Conversion of BLG-NCA over time using NB (red) and PNB_{100} (blue) initiators. The brush-like initiators exhibit remarkable rate acceleration compared with their linear analogues. (C and D) Conversion of BLG-NCA over time using random copolymer P(NB-r-Ph) (C) or block copolymer PNB-b-PPh (D) as initiators. With decreasing density of initiating groups in P(NB-r-Ph), the rate acceleration becomes less significant. In contrast, PNB-b-PPh with different arrangements of initiating sites exhibit similar polymerization kinetics among all four groups, which is attributed to the similar densities of the initiators. (E) Comparison between the conversion of BLG-NCA (black), the increase of the signal of the α-helix from FTIR at 1655 cm^{-1} (green), and the change in ellipticity from CD at 227.9 nm (blue). The secondary, fast polymerization stage coincides with the formation of α-helices as observed by FTIR and CD, suggesting the important role of the helical conformation in the rate acceleration. (F) Scheme illustrating the difference of macrodipoles in linear and brush systems. The close proximity of the initiating groups in the brush system strengthens the interaction between macrodipoles, leading to faster polymerization compared with their linear analogues. Reprinted with permission from ref. 237. Copyright 2017 Springer Nature.
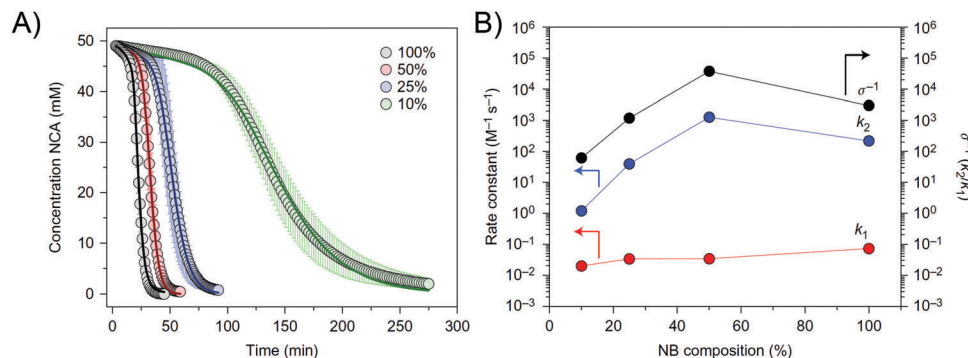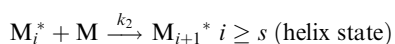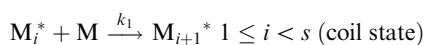
This journal is © The Royal Society of Chemistry 2018

Chem. Soc. Rev., 2018, 47, 7401–7425 | 7419

Fig. 22 Kinetic modeling of the brush polymerization. (A) Kinetic data (circles) obtained from the polymerization of BLG-NCA with PNB-r-PPh macroinitiators are fit with the two-stage kinetic model (solid lines). (B) Extracted rate constants for the primary nucleation stage (k_1) and the second elongation stage (k_2). The density of initiating groups has a greater effect on k_2, which correlates the interaction between macrodipoles with the cooperative growth of polypeptides. Reprinted with permission from ref. 237. Copyright 2017 Springer Nature.

polymers, on the other hand, the packing of α-helices along the PNB backbone further strengthens the electrostatic environment at the polypeptide chain ends, resulting in even faster polymerization.

The macrodipole hypothesis was well supported by the solvent-sensitivity of the brush polymerization. The use of chloroform instead of DCM resulted in even faster polymerization due to the lower dielectric constant of chloroform. However, when *N,N*-dimethylformamide (DMF) was used as the solvent, both the two-stage kinetics and the enhanced rates in brush systems disappeared, as DMF is a well-known polar solvent that interacts with dipoles and breaks the packing between α-helices.

8.3 Kinetic models of cooperative polymerization

The key characteristic of the α-helix involved reaction is that the coil to alpha-helix transition is accompanied by a dramatic rate enhancement, which separates the reaction into two distinct stages. While never described in covalent polymerization previously, the cooperative behavior is well described in the reversible self-assembly of supramolecular molecules.[238–240] A simple two-stage model can be adapted from the nucleation induced cooperative model, with the key feature being irreversible addition of monomers. In the two-stage model, a critical chain length, s, marks the conformation transition of the actively growing chain M_i^* (where i is the DP of the polypeptides) from a coil to a helix, which is accompanied by the switching of the growing rate constant from k_1 to k_2. The cooperativity is defined as $\sigma = k_1/k_2$, with smaller σ indicating stronger cooperative effects.

$$M_i^* + M \xrightarrow{k_1} M_{i+1}^* \ 1 \le i < s \text{ (coil state)}$$

$$M_i^* + M \xrightarrow{k_2} M_{i+1}^* \ i \ge s \text{ (helix state)}$$

The two-stage model was then applied to analyze the polymerization kinetic data generated from the random copolymer scaffolds whose grafting density is controlled by the percentage of NB. The two-stage model was able to fit the experimental data

well (Fig. 22A), and the critical chain length s was determined to be 10 ± 2, which agrees well with the previously reported smallest DP to form stable α-helices.[241] As shown in Fig. 22B, the extracted k_1 remains relatively constant at different grafting densities, indicating that the coupling of amide dipoles within short, coil-like polypeptides has limited impact on the reactions. As a comparison, the density of helices strongly affects k_2. When the fraction of NB was increased from 10% to 50%, k_2 was increased ~1000 times, suggesting the strong effect of the proximity of macrodipoles on the cooperative growth of polypeptides.

9 Conclusions and perspectives

The ability to form ordered secondary structures is a unique feature of synthetic polypeptides compared to conventional polymers. Since the discovery of NCAs in 1906, numerous efforts have been devoted towards the preparation, characterization, and application of synthetic polypeptides. Despite a relatively good understanding of the formation and stabilization of polypeptide conformations, most works have focused on the studies of synthetic polypeptides with random coil structures (*e.g.*, PLG, PLL, and their derivatives). The application of ordered secondary structures, especially α-helices, was limited to water-insoluble polypeptides as the catalysts of stereoselective reactions in the twentieth century. In the past two decades, the development of NCA chemistry has not only provided for functional, well-defined polypeptides which are now accessible to researchers, but, more importantly, has also boosted the discovery of conformation-specific properties of synthetic polypeptides.

This review is aimed at drawing people's attention to the conformation of synthetic polypeptides. Structural differences between the ordered and random-coiled conformation result in completely different behaviors of synthetic polypeptides. For instance, polypeptides with α-helical structures have different sizes, polarities, rigidities, and distributions of side chain functionalities from their random-coiled analogues. As a result, these α-helical polypeptides exhibit beneficial helix-associated

7420 | *Chem. Soc. Rev.*, 2018, **47**, 7401–7425

This journal is © The Royal Society of Chemistry 2018

properties and performances in self-assembly, biomedical application, and polymer synthesis. On the other hand, polypeptides which demonstrate stable β-sheet conformations show strong inter-chain interactions, enabling the formation of gels and amyloid fibrils with good mechanical properties.

The recent discoveries of the conformation-specific properties of synthetic polypeptides, although exciting and inspiring, are still far from matching the functions of naturally occurring proteins. In nature, the functions of proteins are controlled not only by the modulation of their secondary structures, but, more importantly, by the special arrangements of the secondary structures in a three-dimensional space (*i.e.*, tertiary structures and quaternary structures). Thus, the construction of higher ordered structures with synthetic methods, such as the design of complex polymer architectures and the supramolecular assemblies of secondary structures, is a promising direction to further improve the performance of synthetic polypeptides. This requires not only better synthetic control over polypeptide structures, including polydispersity and sequence regularity, but also a deeper understanding of the cooperative behaviors of polypeptides in folding and self-assembly.

At the same time, the large scale production of polypeptide materials is of great interest considering their beneficial properties in self-assembly, catalysis, and biomedical applications. However, the current synthesis and purification of NCA monomers require the use of phosgenation reagents and moisture-free conditions, which greatly limits the commercialization of synthetic polypeptides. Studies to simplify the existing polymerization methods or to find alternative ways to prepare polypeptides are therefore critical for the ultimate realization of polypeptide materials.

Conflicts of interest

There are no conflicts to declare.

Acknowledgements

References

1 D. L. Nelson, A. L. Lehninger and M. M. Cox, *Lehninger Principles of Biochemistry*, W. H. Freeman, New York, 2008.
2 L. Pauling and R. B. Corey, *Proc. Natl. Acad. Sci. U. S. A.*, 1951, **37**, 251–256.
3 L. Pauling, R. B. Corey and H. R. Branson, *Proc. Natl. Acad. Sci. U. S. A.*, 1951, **37**, 205–211.
4 K. Henzler-Wildman and D. Kern, *Nature*, 2007, **450**, 964–972.
5 A. R. Means, M. F. VanBerkum, I. Bagchi, K. P. Lu and C. D. Rasmussen, *Pharmacol. Ther.*, 1991, **50**, 255–270.
6 M. Zhang, T. Tanaka and M. Ikura, *Nat. Struct. Biol.*, 1995, **2**, 758–767.
7 R. P. Cheng, S. H. Gellman and W. F. DeGrado, *Chem. Rev.*, 2001, **101**, 3219–3232.
8 D. Seebach and J. Gardiner, *Acc. Chem. Res.*, 2008, **41**, 1366–1375.
9 D. Zhang, S. H. Lahasky, L. Guo, C. U. Lee and M. Lavan, *Macromolecules*, 2012, **45**, 5833–5841.
10 J. Sun and R. N. Zuckermann, *ACS Nano*, 2013, **7**, 4715–4732.
11 N. Gangloff, J. Ulbricht, T. Lorson, H. Schlaad and R. Luxenhofer, *Chem. Rev.*, 2016, **116**, 1753–1802.
12 S. H. Gellman, *Acc. Chem. Res.*, 1998, **31**, 173–180.
13 D. J. Hill, M. J. Mio, R. B. Prince, T. S. Hughes and J. S. Moore, *Chem. Rev.*, 2001, **101**, 3893–4012.
14 J. Clayden, *Chem. Soc. Rev.*, 2009, **38**, 817–829.
15 T. A. Martinek and F. Fulop, *Chem. Soc. Rev.*, 2012, **41**, 687–702.
16 R. B. Merrifield, *J. Am. Chem. Soc.*, 1963, **85**, 2149–2154.
17 J. C. van Hest and D. A. Tirrell, *Chem. Commun.*, 2001, 1897–1904.
18 H. Leuchs, *Ber. Dtsch. Chem. Ges.*, 1906, **39**, 857–861.
19 C. Bonduelle, *Polym. Chem.*, 2018, **9**, 1517–1529.
20 N. Hadjichristidis, H. Iatrou, M. Pitsikalis and G. Sakellariou, *Chem. Rev.*, 2009, **109**, 5528–5578.
21 T. J. Deming, *Chem. Rev.*, 2016, **116**, 786–808.
22 A. Carlsen and S. Lecommandoux, *Curr. Opin. Colloid Interface Sci.*, 2009, **14**, 329–339.
23 H. Lu, J. Wang, Z. Song, L. Yin, Y. Zhang, H. Tang, C. Tu, Y. Lin and J. Cheng, *Chem. Commun.*, 2014, **50**, 139–155.
24 J. Huang and A. Heise, *Chem. Soc. Rev.*, 2013, **42**, 7373–7390.
25 Y. Shen, X. Fu, W. Fu and Z. Li, *Chem. Soc. Rev.*, 2015, **44**, 612–622.
26 S. H. Wibowo, A. Sulistio, E. H. Wong, A. Blencowe and G. G. Qiao, *Chem. Commun.*, 2014, **50**, 4971–4988.
27 T. Borase and A. Heise, *Adv. Mater.*, 2016, **28**, 5725–5731.
28 T. J. Deming, *Adv. Drug Delivery Rev.*, 2002, **54**, 1145–1155.
29 T. J. Deming, *Prog. Polym. Sci.*, 2007, **32**, 858–875.
30 K. Kataoka, A. Harada and Y. Nagasaki, *Adv. Drug Delivery Rev.*, 2012, **64**, 37–48.
31 C. Deng, J. Wu, R. Cheng, F. Meng, H.-A. Klok and Z. Zhong, *Prog. Polym. Sci.*, 2014, **39**, 330–364.
32 R. Zhang, Z. Song, L. Yin, N. Zheng, H. Tang, H. Lu, N. P. Gabrielson, Y. Lin, K. Kim and J. Cheng, *Wiley Interdiscip. Rev.: Nanomed. Nanobiotechnol.*, 2015, **7**, 98–110.
33 Z. Song, Z. Han, S. Lv, C. Chen, L. Chen, L. Yin and J. Cheng, *Chem. Soc. Rev.*, 2017, **46**, 6570–6599.
34 K. T. Oneil and W. F. Degrado, *Science*, 1990, **250**, 646–651.
35 C. A. Kim and J. M. Berg, *Nature*, 1993, **362**, 267–270.
36 R. L. Baldwin, *Biophys. Chem.*, 1995, **55**, 127–135.
37 J. M. Scholtz, H. Qian, V. H. Robbins and R. L. Baldwin, *Biochemistry*, 1993, **32**, 9668–9676.
38 A. Chakrabartty, A. J. Doig and R. L. Baldwin, *Proc. Natl. Acad. Sci. U. S. A.*, 1993, **90**, 11332–11336.
39 P. Doty, A. Wada, J. T. Yang and E. R. Blout, *J. Polym. Sci.*, 1957, **23**, 851–861.

40 S. Ikeda, *Biopolymers*, 1967, **5**, 359–374.

41 L. Yin, H. Tang, K. H. Kim, N. Zheng, Z. Song, N. P. Gabrielson, H. Lu and J. Cheng, *Angew. Chem., Int. Ed.*, 2013, **52**, 9182–9186.

42 M. Xiong, Y. Bao, X. Xu, H. Wang, Z. Han, Z. Wang, Y. Liu, S. Huang, Z. Song, J. Chen, R. M. Peek Jr., L. Yin, L.-F. Chen and J. Cheng, *Proc. Natl. Acad. Sci. U. S. A.*, 2017, **114**, 12675–12680.

43 S. L. Perry, L. Leon, K. Q. Hoffmann, M. J. Kade, D. Priftis, K. A. Black, D. Wong, R. A. Klein, C. F. Pierce, K. O. Margossian, J. K. Whitmer, J. Qin, J. J. de Pablo and M. Tirrell, *Nat. Commun.*, 2015, **6**, 6052.

44 Y. Sun, A. L. Wollenberg, T. M. O'Shea, Y. Cui, Z. H. Zhou, M. V. Sofroniew and T. J. Deming, *J. Am. Chem. Soc.*, 2017, **139**, 15114–15121.

45 J. S. Albert and A. D. Hamilton, *Biochemistry*, 1995, **34**, 984–990.

46 S. E. Ostroy, N. Lotan, R. T. Ingwall and H. A. Scheraga, *Biopolymers*, 1970, **9**, 749–764.

47 S. Kubota and G. Fasman, *J. Am. Chem. Soc.*, 1974, **96**, 4684–4686.

48 N. Lotan, A. Yaron and A. Berger, *Biopolymers*, 1966, **4**, 365–368.

49 H. Lu, J. Wang, Y. Bai, J. W. Lang, S. Liu, Y. Lin and J. Cheng, *Nat. Commun.*, 2011, **2**, 206.

50 R. Mildner and H. Menzel, *Biomacromolecules*, 2014, **15**, 4528–4533.

51 R. A. Mansbach and A. L. Ferguson, *J. Chem. Phys.*, 2015, **142**, 105101.

52 B. M. P. Huyghues-Despointes, T. M. Klingler and R. L. Baldwin, *Biochemistry*, 1995, **34**, 13267–13271.

53 Z. Song, R. A. Mansbach, H. He, K.-C. Shih, R. Baumgartner, N. Zheng, X. Ba, Y. Huang, D. Mani, Y. Liu, Y. Lin, M.-P. Nieh, A. L. Ferguson, L. Yin and J. Cheng, *Nat. Commun.*, 2017, **8**, 92.

54 S. Marqusee and R. L. Baldwin, *Proc. Natl. Acad. Sci. U. S. A.*, 1987, **84**, 8898–8902.

55 M. Yu, A. P. Nowak, T. J. Deming and D. J. Pochan, *J. Am. Chem. Soc.*, 1999, **121**, 12210–12211.

56 A. C. Engler, H. I. Lee and P. T. Hammond, *Angew. Chem., Int. Ed.*, 2009, **48**, 9334–9338.

57 C. Chen, Z. Wang and Z. Li, *Biomacromolecules*, 2011, **12**, 2859–2863.

58 M. Zhu, Y. Wu, C. Ge, Y. Ling and H. Tang, *Macromolecules*, 2016, **49**, 3542–3549.

59 J. Yan, K. Liu, W. Li, H. Shi and A. Zhang, *Macromolecules*, 2016, **49**, 510–517.

60 J. R. Kramer and T. J. Deming, *J. Am. Chem. Soc.*, 2010, **132**, 15068–15071.

61 Y. Zhang, H. Lu, Y. Lin and J. Cheng, *Macromolecules*, 2011, **44**, 6641–6644.

62 N. P. Gabrielson, H. Lu, L. Yin, D. Li, F. Wang and J. Cheng, *Angew. Chem., Int. Ed.*, 2012, **51**, 1143–1147.

63 Z. Song, N. Zheng, X. Ba, L. Yin, R. Zhang, L. Ma and J. Cheng, *Biomacromolecules*, 2014, **15**, 1491–1497.

64 R. Zhang, N. Zheng, Z. Song, L. Yin and J. Cheng, *Biomaterials*, 2014, **35**, 3443–3454.

65 M. Xiong, M. W. Lee, R. A. Mansbach, Z. Song, Y. Bao, R. M. Peek Jr., C. Yao, L.-F. Chen, A. L. Ferguson, G. C. Wong and J. Cheng, *Proc. Natl. Acad. Sci. U. S. A.*, 2015, **112**, 13155–13160.

66 H. Tang, L. Yin, H. Lu and J. Cheng, *Biomacromolecules*, 2012, **13**, 2609–2615.

67 M. Nguyen, J. L. Stigliani, G. Pratviel and C. Bonduelle, *Chem. Commun.*, 2017, **53**, 7501–7504.

68 K.-S. Krannig and H. Schlaad, *J. Am. Chem. Soc.*, 2012, **134**, 18542–18545.

69 M. Xiong, Z. Han, Z. Song, J. Yu, H. Ying, L. Yin and J. Cheng, *Angew. Chem., Int. Ed.*, 2017, **56**, 10826–10829.

70 Z. Song, H. Kim, X. Ba, R. Baumgartner, J. S. Lee, H. Tang, C. Leal and J. Cheng, *Soft Matter*, 2015, **11**, 4091–4098.

71 C. Bonduelle, F. Makni, L. Severac, E. Piedra-Arroni, C.-L. Serpentini, S. Lecommandoux and G. Pratviel, *RSC Adv.*, 2016, **6**, 84694–84697.

72 J. Yuan, Y. Zhang, Y. Sun, Z. Cai, L. Yang and H. Lu, *Biomacromolecules*, 2018, **19**, 2089–2097.

73 V. K. Kotharangannagari, A. Sánchez-Ferrer, J. Ruokolainen and R. Mezzenga, *Macromolecules*, 2011, **44**, 4569–4573.

74 J. R. Kramer and T. J. Deming, *J. Am. Chem. Soc.*, 2014, **136**, 5547–5550.

75 J. Yan, K. Liu, X. Zhang, W. Li and A. Zhang, *J. Polym. Sci., Part A: Polym. Chem.*, 2015, **53**, 33–41.

76 G. E. Negri and T. J. Deming, *ACS Macro Lett.*, 2016, **5**, 1253–1256.

77 E. Piedra-Arroni, F. Makni, L. Severac, J.-L. Stigliani, G. Pratviel and C. Bonduelle, *Polymers*, 2017, **9**, 276.

78 J. R. Kramer and T. J. Deming, *J. Am. Chem. Soc.*, 2012, **134**, 4112–4115.

79 J. A. Schellman, *J. Phys. Chem.*, 1958, **62**, 1485–1494.

80 J. H. Gibbs and E. A. DiMarzio, *J. Chem. Phys.*, 1959, **30**, 271–282.

81 B. H. Zimm and J. K. Bragg, *J. Chem. Phys.*, 1959, **31**, 526–535.

82 S. Lifson and A. Roig, *J. Chem. Phys.*, 1961, **34**, 1963–1974.

83 K. Nagai, *J. Phys. Soc. Jpn.*, 1960, **15**, 407–416.

84 P. Papadopoulos, G. Floudas, H.-A. Klok, I. Schnell and T. Pakula, *Biomacromolecules*, 2004, **5**, 81–91.

85 G. Floudas and H. W. Spiess, *Macromol. Rapid Commun.*, 2009, **30**, 278–298.

86 Y. Ren, H. Fu, R. Baumgartner, Y. Zhang, J. Cheng and Y. Lin, *ACS Macro Lett.*, 2017, **6**, 733–737.

87 Y. Ren, R. Baumgartner, H. Fu, P. van der Schoot, J. Cheng and Y. Lin, *Biomacromolecules*, 2017, **18**, 2324–2332.

88 J. Wang, H. Lu, Y. Ren, Y. Zhang, M. Morton, J. Cheng and Y. Lin, *Macromolecules*, 2011, **44**, 8699–8708.

89 K. Ghosh and K. A. Dill, *J. Am. Chem. Soc.*, 2009, **131**, 2306–2312.

90 E. G. Bellomo, M. D. Wyrsta, L. Pakstis, D. J. Pochan and T. J. Deming, *Nat. Mater.*, 2004, **3**, 244–248.

91 E. P. Holowka, D. J. Pochan and T. J. Deming, *J. Am. Chem. Soc.*, 2005, **127**, 12423–12428.

92 E. P. Holowka, V. Z. Sun, D. T. Kamei and T. J. Deming, *Nat. Mater.*, 2007, **6**, 52–57.

93   A. R. Rodriguez, J. R. Kramer and T. J. Deming, *Biomacromolecules*, 2013, **14**, 3610–3614.

94   U. J. Choe, A. R. Rodriguez, B. S. Lee, S. M. Knowles, A. M. Wu, T. J. Deming and D. T. Kamei, *Biomacromolecules*, 2013, **14**, 1458–1464.

95   B. S. Lee, A. T. Yip, A. V. Thach, A. R. Rodriguez, T. J. Deming and D. T. Kamei, *Int. J. Pharm.*, 2015, **496**, 903–911.

96   A. R. Rodriguez, U. J. Choe, D. T. Kamei and T. J. Deming, *Macromol. Biosci.*, 2015, **15**, 90–97.

97   C. F. Ajibola, S. A. Malomo, T. N. Fagbemi and R. E. Aluko, *Food Hydrocolloids*, 2016, **56**, 189–200.

98   M. Lukic, I. Pantelic and S. Savic, *Tenside, Surfactants, Deterg.*, 2016, **53**, 7–19.

99   D. Priftis, K. Megley, N. Laugel and M. Tirrell, *J. Colloid Interface Sci.*, 2013, **398**, 39–50.

100 D. Priftis, L. Leon, Z. Song, S. L. Perry, K. O. Margossian, A. Tropnikova, J. Cheng and M. Tirrell, *Angew. Chem., Int. Ed.*, 2015, **54**, 11128–11132.

101 A. P. Nowak, V. Breedveld, L. Pakstis, B. Ozbas, D. J. Pine, D. Pochan and T. J. Deming, *Nature*, 2002, **417**, 424–428.

102 A. P. Nowak, V. Breedveld, D. J. Pine and T. J. Deming, *J. Am. Chem. Soc.*, 2003, **125**, 15666–15670.

103 T. J. Deming, *Wiley Interdiscip. Rev.: Nanomed. Nanobiotechnol.*, 2014, **6**, 283–297.

104 A. R. Rodriguez, U. J. Choe, D. T. Kamei and T. J. Deming, *Macromol. Biosci.*, 2012, **12**, 805–811.

105 Y. Y. Choi, M. K. Joo, Y. S. Sohn and B. Jeong, *Soft Matter*, 2008, **4**, 2383–2387.

106 F. Hermes, K. Otte, J. Brandt, M. Gräwert, H. G. Börner and H. Schlaad, *Macromolecules*, 2011, **44**, 7489–7492.

107 Y. Mochida, H. Cabral, Y. Miura, F. Albertini, S. Fukushima, K. Osada, N. Nishiyama and K. Kataoka, *ACS Nano*, 2014, **8**, 6724–6738.

108 A. Koide, A. Kishimura, K. Osada, W.-D. Jang, Y. Yamasaki and K. Kataoka, *J. Am. Chem. Soc.*, 2006, **128**, 5988–5989.

109 U. J. Choe, A. R. Rodriguez, Z. Li, S. Boyarskiy, T. J. Deming and D. T. Kamei, *Macromol. Chem. Phys.*, 2013, **214**, 994–999.

110 A. M. Jonker, D. W. P. M. Löwik and J. C. M. van Hest, *Chem. Mater.*, 2012, **24**, 759–773.

111 N. A. Peppas, Y. Huang, M. Torres-Lugo, J. H. Ward and J. Zhang, *Annu. Rev. Biomed. Eng.*, 2000, **2**, 9–29.

112 C. Yan and D. J. Pochan, *Chem. Soc. Rev.*, 2010, **39**, 3528–3540.

113 H. J. Oh, M. K. Joo, Y. S. Sohn and B. Jeong, *Macromolecules*, 2008, **41**, 8204–8209.

114 H. Li, N. R. Johnson, A. Usas, A. Lu, M. Poddar, Y. Wang and J. Huard, *Stem Cells Transl. Med.*, 2013, **2**, 667–677.

115 H. J. Kim, B. H. Choi, S. H. Jun and H. J. Cha, *Adv. Healthcare Mater.*, 2016, **5**, 3191–3202.

116 F. W. Tiebackx, *Z. Chem. Ind. Kolloide*, 1911, **8**, 198–201.

117 J. T. Overbeek and M. J. Voorn, *J. Cell. Comp. Physiol.*, 1957, **49**, 7–22; discussion, 22–26.

118 C. G. de Kruif, F. Weinbreck and R. de Vries, *Curr. Opin. Colloid Interface Sci.*, 2004, **9**, 340–349.

119 D. Sept and J. A. McCammon, *Biophys. J.*, 2001, **81**, 667–674.

120 T. O. Yeates and J. E. Padilla, *Curr. Opin. Struct. Biol.*, 2002, **12**, 464–470.

121 J. Wang, H. Lu, R. Kamat, S. V. Pingali, V. S. Urban, J. Cheng and Y. Lin, *J. Am. Chem. Soc.*, 2011, **133**, 12906–12909.

122 J. Li, Y. Gao, Y. Kuang, J. Shi, X. Du, J. Zhou, H. Wang, Z. Yang and B. Xu, *J. Am. Chem. Soc.*, 2013, **135**, 9907–9914.

123 P. J. Flory, *Proc. R. Soc. London, Ser. A*, 1956, **234**, 73–89.

124 A. Elliott and E. J. Ambrose, *Discuss. Faraday Soc.*, 1950, **9**, 246–251.

125 C. Robinson, *Trans. Faraday Soc.*, 1956, **52**, 571–592.

126 D. L. Patel and D. B. Dupré, *J. Chem. Phys.*, 1980, **72**, 2515–2524.

127 I. Uematsu and Y. Uematsu, in *Liquid Crystal Polymers I*, ed. N. A. Platé, Springer Berlin Heidelberg, Berlin, Heidelberg, 1984, pp. 37–73.

128 W. G. Miller, L. Kou, K. Tohyama and V. Voltaggio, *J. Polym. Sci., Part C: Polym. Symp.*, 1978, **65**, 91–106.

129 M. M. Giraud-Guille, L. Besseau and R. Martin, *J. Biomech.*, 2003, **36**, 1571–1579.

130 R. Huang, Y. Wang, W. Qi, R. Su and Z. He, *Nanoscale Res. Lett.*, 2014, **9**, 653.

131 Y. Engelborghs, R. Audenaert, L. Heremans and K. Heremans, in *Cytoskeletal and Extracellular Proteins*, ed. U. Aebi and J. Engel, Springer Berlin Heidelberg, Berlin, Heidelberg, 1989, pp. 222–224.

132 F. Oosawa and M. Kasai, *J. Mol. Biol.*, 1962, **4**, 10–21.

133 R. Audenaert, L. Heremans, K. Heremans and Y. Engelborghs, *Biochim. Biophys. Acta, Protein Struct. Mol. Enzymol.*, 1989, **996**, 110–115.

134 E. D. Korn, M. F. Carlier and D. Pantaloni, *Science*, 1987, **238**, 638–644.

135 X. Zheng, K. Diraviyam and D. Sept, *Biophys. J.*, 2007, **93**, 1277–1283.

136 J. Zhou, X. Du, C. Berciu, H. He, J. Shi, D. Nicastro and B. Xu, *Chem*, 2016, **1**, 246–263.

137 Z. Yang, G. Liang and B. Xu, *Acc. Chem. Res.*, 2008, **41**, 315–326.

138 K. Thornton, A. M. Smith, C. L. Merry and R. V. Ulijn, *Biochem. Soc. Trans.*, 2009, **37**, 660–664.

139 J. Gao, W. Zheng, D. Kong and Z. Yang, *Soft Matter*, 2011, **7**, 10443–10448.

140 X. Du, J. Zhou, J. Shi and B. Xu, *Chem. Rev.*, 2015, **115**, 13165–13307.

141 Z. M. Yang, K. M. Xu, Z. F. Guo, Z. H. Guo and B. Xu, *Adv. Mater.*, 2007, **19**, 3152–3156.

142 A. K. Das, R. Collins and R. V. Ulijn, *Small*, 2008, **4**, 279–287.

143 Z. Yang, P.-L. Ho, G. Liang, K. H. Chow, Q. Wang, Y. Cao, Z. Guo and B. Xu, *J. Am. Chem. Soc.*, 2007, **129**, 266–267.

144 Y. Liu, V. Javvaji, S. R. Raghavan, W. E. Bentley and G. F. Payne, *J. Agric. Food Chem.*, 2012, **60**, 8963–8967.

145 L. Chronopoulou, S. Lorenzoni, G. Masci, M. Dentini, A. R. Togna, G. Togna, F. Bordi and C. Palocci, *Soft Matter*, 2010, **6**, 2525–2532.

146 H. Xia, H. Fu, Y. Zhang, K.-C. Shih, Y. Ren, M. Anuganti, M.-P. Nieh, J. Cheng and Y. Lin, *J. Am. Chem. Soc.*, 2017, **139**, 11106–11116.

147 K. Inoue, N. Baden and M. Terazima, *J. Phys. Chem. B*, 2005, **109**, 22623–22628.

148 J. Rodríguez-Hernández and S. Lecommandoux, *J. Am. Chem. Soc.*, 2005, **127**, 2026–2027.

149 S. Ihara, T. Ooi and S. Takahashi, *Biopolymers*, 1982, **21**, 131–145.

150 B. Ozbas, J. Kretsinger, K. Rajagopal, J. P. Schneider and D. J. Pochan, *Macromolecules*, 2004, **37**, 7331–7337.

151 K. Osada, H. Cabral, Y. Mochida, S. Lee, K. Nagata, T. Matsuura, M. Yamamoto, Y. Anraku, A. Kishimura, N. Nishiyama and K. Kataoka, *J. Am. Chem. Soc.*, 2012, **134**, 13172–13175.

152 F. Chiti and C. M. Dobson, *Annu. Rev. Biochem.*, 2006, **75**, 333–366.

153 M. Fandrich, *Cell. Mol. Life Sci.*, 2007, **64**, 2066–2078.

154 T. P. Knowles and R. Mezzenga, *Adv. Mater.*, 2016, **28**, 6546–6561.

155 C. B. Caputo, I. R. Sobel, L. A. Sygowski, R. A. Lampe and R. C. Spreen, *Arch. Biochem. Biophys.*, 1993, **306**, 321–330.

156 A. H. DePace, A. Santoso, P. Hillner and J. S. Weissman, *Cell*, 1998, **93**, 1241–1252.

157 M. López de la Paz and L. Serrano, *Proc. Natl. Acad. Sci. U. S. A.*, 2004, **101**, 87–92.

158 M. Fandrich and C. M. Dobson, *EMBO J.*, 2002, **21**, 5682–5690.

159 F. Bai, C. Zeng, S. Yang, Y. Zhang, Y. He and J. Jin, *Biochem. Biophys. Res. Commun.*, 2008, **369**, 830–834.

160 J. Lai, W. Fu, L. Zhu, R. Guo, D. Liang, Z. Li and Y. Huang, *Langmuir*, 2014, **30**, 7221–7226.

161 J. Lai, C. Zheng, D. Liang and Y. Huang, *Biomacromolecules*, 2013, **14**, 4515–4519.

162 K. Cieślik-Boczula, *Biochimie*, 2017, **137**, 106–114.

163 A. Fulara and W. Dzwolak, *J. Phys. Chem. B*, 2010, **114**, 8278–8283.

164 A. Fulara, A. Lakhani, S. Wójcik, H. Nieznańska, T. A. Keiderling and W. Dzwolak, *J. Phys. Chem. B*, 2011, **115**, 11010–11016.

165 A. Fulara, A. Hernik, H. Nieznańska and W. Dzwolak, *PLoS One*, 2014, **9**, e105660.

166 Y. Yamaoki, H. Imamura, A. Fulara, S. Wójcik, L. Bożycki, M. Kato, T. A. Keiderling and W. Dzwolak, *J. Phys. Chem. B*, 2012, **116**, 5172–5178.

167 A. Hernik, W. Pulawski, B. Fedorczyk, D. Tymecka, A. Misicka, S. Filipek and W. Dzwolak, *Langmuir*, 2015, **31**, 10500–10507.

168 A. Hernik-Magoń, W. Puławski, B. Fedorczyk, D. Tymecka, A. Misicka, P. Szymczak and W. Dzwolak, *Biomacromolecules*, 2016, **17**, 1376–1382.

169 M. R. Sawaya, S. Sambashivan, R. Nelson, M. I. Ivanova, S. A. Sievers, M. I. Apostol, M. J. Thompson, M. Balbirnie, J. J. Wiltzius, H. T. McFarlane, A. Ø. Madsen, C. Riekel and D. Eisenberg, *Nature*, 2007, **447**, 453–457.

170 C. Wasmer, A. Lange, H. Van Melckebeke, A. B. Siemer, R. Riek and B. H. Meier, *Science*, 2008, **319**, 1523–1526.

171 A. W. Fitzpatrick, G. T. Debelouchina, M. J. Bayro, D. K. Clare, M. A. Caporini, V. S. Bajaj, C. P. Jaroniec, L. Wang, V. Ladizhansky, S. A. Muller, C. E. MacPhee, C. A. Waudby, H. R. Mott, A. De Simone, T. P. Knowles, H. R. Saibil, M. Vendruscolo, E. V. Orlova, R. G. Griffin and C. M. Dobson, *Proc. Natl. Acad. Sci. U. S. A.*, 2013, **110**, 5468–5473.

172 T. P. Knowles, A. W. Fitzpatrick, S. Meehan, H. R. Mott, M. Vendruscolo, C. M. Dobson and M. E. Welland, *Science*, 2007, **318**, 1900–1903.

173 T. P. Knowles and M. J. Buehler, *Nat. Nanotechnol.*, 2011, **6**, 469–479.

174 M. R. Chapman, L. S. Robinson, J. S. Pinkner, R. Roth, J. Heuser, M. Hammar, S. Normark and S. J. Hultgren, *Science*, 2002, **295**, 851–855.

175 V. A. Iconomidou, G. Vriend and S. J. Hamodrakas, *FEBS Lett.*, 2000, **479**, 141–145.

176 A. S. Mostaert, M. J. Higgins, T. Fukuma, F. Rindi and S. P. Jarvis, *J. Biol. Phys.*, 2006, **32**, 393–401.

177 S. K. Maji, D. Schubert, C. Rivier, S. Lee, J. E. Rivier and R. Riek, *PLoS Biol.*, 2008, **6**, e17.

178 C. Li, J. Adamcik and R. Mezzenga, *Nat. Nanotechnol.*, 2012, **7**, 421–427.

179 C. Li, S. Bolisetty and R. Mezzenga, *Adv. Mater.*, 2013, **25**, 3694–3700.

180 S. Kasai, Y. Ohga, M. Mochizuki, N. Nishi, Y. Kadoya and M. Nomizu, *Biopolymers*, 2004, **76**, 27–33.

181 D. Men, Y.-C. Guo, Z.-P. Zhang, H.-P. Wei, Y.-F. Zhou, Z.-Q. Cui, X.-S. Liang, K. Li, Y. Leng, X.-Y. You and X.-E. Zhang, *Nano Lett.*, 2009, **9**, 2246–2250.

182 D. Men, Z.-P. Zhang, Y.-C. Guo, D.-H. Zhu, L.-J. Bi, J.-Y. Deng, Z.-Q. Cui, H.-P. Wei and X.-E. Zhang, *Biosens. Bioelectron.*, 2010, **26**, 1137–1141.

183 M. Reches and E. Gazit, *Science*, 2003, **300**, 625–627.

184 W. Dzwolak, *Biochemistry*, 2007, **46**, 1568–1572.

185 S. Bolisetty, J. J. Vallooran, J. Adamcik, S. Handschin, F. Gramm and R. Mezzenga, *J. Colloid Interface Sci.*, 2011, **361**, 90–96.

186 T. Scheibel, R. Parthasarathy, G. Sawicki, X.-M. Lin, H. Jaeger and S. L. Lindquist, *Proc. Natl. Acad. Sci. U. S. A.*, 2003, **100**, 4527–4532.

187 A. Herland, P. Björk, K. P. R. Nilsson, J. D. M. Olsson, P. Åsberg, P. Konradsson, P. Hammarström and O. Inganäs, *Adv. Mater.*, 2005, **17**, 1466–1471.

188 H. Tanaka, A. Herland, L. J. Lindgren, T. Tsutsui, M. R. Andersson and O. Inganas, *Nano Lett.*, 2008, **8**, 2858–2861.

189 S. Barrau, F. Zhang, A. Herland, W. Mammo, M. R. Andersson and O. Inganäs, *Appl. Phys. Lett.*, 2008, **93**, 023307.

190 Y. Liang, P. Guo, S. V. Pingali, S. Pabit, P. Thiyagarajan, K. M. Berland and D. G. Lynn, *Chem. Commun.*, 2008, 6522–6524.

191 A. Rizzo, N. Solin, L. J. Lindgren, M. R. Andersson and O. Inganäs, *Nano Lett.*, 2010, **10**, 2225–2230.

192 K. Kataoka, G. S. Kwon, M. Yokoyama, T. Okano and Y. Sakurai, *J. Controlled Release*, 1993, **24**, 119–132.

193 Y. Hou, J. Yuan, Y. Zhou, J. Yu and H. Lu, *J. Am. Chem. Soc.*, 2016, **138**, 10995–11000.

7424 | *Chem. Soc. Rev.*, 2018, **47**, 7401–7425

This journal is © The Royal Society of Chemistry 2018

194 Y. Hou, Y. Zhou, H. Wang, R. Wang, J. Yuan, Y. Hu, K. Sheng, J. Feng, S. Yang and H. Lu, *J. Am. Chem. Soc.*, 2018, **140**, 1170–1178.

195 K. N. Sill, B. Sullivan, A. Carie and J. E. Semple, *Biomacromolecules*, 2017, **18**, 1874–1884.

196 K. Miyata, N. Nishiyama and K. Kataoka, *Chem. Soc. Rev.*, 2012, **41**, 2562–2574.

197 J. Yen, Y. Zhang, N. P. Gabrielson, L. Yin, L. Guan, I. Chaudhury, H. Lu, F. Wang and J. Cheng, *Biomater. Sci.*, 2013, **1**, 719–727.

198 L. Yin, Z. Song, K. H. Kim, N. Zheng, N. P. Gabrielson and J. Cheng, *Adv. Mater.*, 2013, **25**, 3063–3070.

199 L. Yin, Z. Song, K. H. Kim, N. Zheng, H. Tang, H. Lu, N. P. Gabrielson and J. Cheng, *Biomaterials*, 2013, **34**, 2340–2349.

200 L. Yin, Z. Song, Q. Qu, K. H. Kim, N. Zheng, C. Yao, I. Chaudhury, H. Tang, N. P. Gabrielson, F. M. Uckun and J. Cheng, *Angew. Chem., Int. Ed.*, 2013, **52**, 5757–5761.

201 N. Zheng, L. Yin, Z. Song, L. Ma, H. Tang, N. P. Gabrielson, H. Lu and J. Cheng, *Biomaterials*, 2014, **35**, 1302–1314.

202 N. Zheng, Z. Song, Y. Liu, R. Zhang, R. Zhang, C. Yao, F. M. Uckun, L. Yin and J. Cheng, *J. Controlled Release*, 2015, **205**, 231–239.

203 J. Yen, H. Ying, H. Wang, L. Yin, F. Uckun and J. Cheng, *ACS Biomater. Sci. Eng.*, 2016, **2**, 326–335.

204 N. Zheng, Z. Song, Y. Liu, L. Yin and J. Cheng, *Front. Chem. Sci. Eng.*, 2017, **11**, 521–528.

205 N. Zheng, Z. Song, J. Yang, Y. Liu, F. Li, J. Cheng and L. Yin, *Acta Biomater.*, 2017, **58**, 146–157.

206 H.-X. Wang, Z. Song, Y.-H. Lao, X. Xu, J. Gong, D. Cheng, S. Chakraborty, J. S. Park, M. Li, D. Huang, L. Yin, J. Cheng and K. W. Leong, *Proc. Natl. Acad. Sci. U. S. A.*, 2018, **115**, 4903–4908.

207 H. Tang, L. Yin, K. H. Kim and J. Cheng, *Chem. Sci.*, 2013, **4**, 3839–3844.

208 M. W. Lee, M. Han, G. V. Bossa, C. Snell, Z. Song, H. Tang, L. Yin, J. Cheng, S. May, E. Luijten and G. C. Wong, *ACS Nano*, 2017, **11**, 2858–2871.

209 M. Zasloff, *Nature*, 2002, **415**, 389–395.

210 R. E. Hancock and H. G. Sahl, *Nat. Biotechnol.*, 2006, **24**, 1551–1557.

211 L. Yang, V. D. Gordon, D. R. Trinkle, N. W. Schmidt, M. A. Davis, C. DeVries, A. Som, J. E. Cronan Jr., G. N. Tew and G. C. Wong, *Proc. Natl. Acad. Sci. U. S. A.*, 2008, **105**, 20595–20600.

212 J. G. Hurdle, A. J. O'Neill, I. Chopra and R. E. Lee, *Nat. Rev. Microbiol.*, 2011, **9**, 62–75.

213 A. C. Engler, N. Wiradharma, Z. Y. Ong, D. J. Coady, J. L. Hedrick and Y.-Y. Yang, *Nano Today*, 2012, **7**, 201–222.

214 Y. Chen, C. T. Mant, S. W. Farmer, R. E. Hancock, M. L. Vasil and R. S. Hodges, *J. Biol. Chem.*, 2005, **280**, 12316–12329.

215 H. Meng and K. Kumar, *J. Am. Chem. Soc.*, 2007, **129**, 15615–15622.

216 M. J. Porter and J. Skidmore, *Chem. Commun.*, 2000, 1215–1225.

217 Y. Zhu, Q. Wang, R. G. Cornwall and Y. Shi, *Chem. Rev.*, 2014, **114**, 8199–8256.

218 S. Julia, J. Masana and J. C. Vega, *Angew. Chem., Int. Ed.*, 1980, **19**, 929–931.

219 S. Juliá, J. Guixer, J. Masana, J. Rocas, S. Colonna, R. Annuziata and H. Molinari, *J. Chem. Soc., Perkin Trans. 1*, 1982, 1317–1324.

220 S. Colonna, H. Molinari, S. Banfi, S. Juliá, J. Masana and A. Alvarez, *Tetrahedron*, 1983, **39**, 1635–1641.

221 S. Banfi, S. Colonna, H. Molinari, S. Julia and J. Guixer, *Tetrahedron*, 1984, **40**, 5207–5211.

222 P. A. Bentley, S. Bergeron, M. W. Cappi, D. E. Hibbs, M. B. Hursthouse, T. C. Nugent, R. Pulido, S. M. Roberts and L. Eduardo Wu, *Chem. Commun.*, 1997, 739–740.

223 R. W. Flood, T. P. Geller, S. A. Petty, S. M. Roberts, J. Skidmore and M. Volk, *Org. Lett.*, 2001, **3**, 683–686.

224 C. Berube, X. Barbeau, P. Lague and N. Voyer, *Chem. Commun.*, 2017, **53**, 5099–5102.

225 T. Geller, A. Gerlach, C. M. Krüger and H. C. Militzer, *Tetrahedron Lett.*, 2004, **45**, 5065–5067.

226 S. Itsuno, M. Sakakura and K. Ito, *J. Org. Chem.*, 1990, **55**, 6047–6049.

227 P. A. Bentley, M. W. Cappi, R. W. Flood, S. M. Roberts and J. A. Smith, *Tetrahedron Lett.*, 1998, **39**, 9297–9300.

228 R. Takagi, A. Shiraki, T. Manabe, S. Kojima and K. Ohkata, *Chem. Lett.*, 2000, 366–367.

229 A. Berkessel, N. Gasch, K. Glaubitz and C. Koch, *Org. Lett.*, 2001, **3**, 3839–3842.

230 D. R. Kelly, T. T. T. Bui, E. Caroff, A. F. Drake and S. M. Roberts, *Tetrahedron Lett.*, 2004, **45**, 3885–3888.

231 D. R. Kelly and S. M. Roberts, *Chem. Commun.*, 2004, 2018–2020.

232 J. Lüders and T. Stearns, *Nat. Rev. Mol. Cell Biol.*, 2007, **8**, 161–167.

233 R. Dominguez and K. C. Holmes, *Annu. Rev. Biophys.*, 2011, **40**, 169–186.

234 D. G. Ballard and C. H. Bamford, *Nature*, 1953, **172**, 907–908.

235 P. Doty and R. D. Lundberg, *J. Am. Chem. Soc.*, 1956, **78**, 4810–4812.

236 R. D. Lundberg and P. Doty, *J. Am. Chem. Soc.*, 1957, **79**, 3961–3972.

237 R. Baumgartner, H. Fu, Z. Song, Y. Lin and J. Cheng, *Nat. Chem.*, 2017, **9**, 614–622.

238 F. Oosawa and S. Asakura, *Thermodynamics of the polymerization of protein*, Academic Press, London, New York, 1975.

239 D. H. Zhao and J. S. Moore, *Org. Biomol. Chem.*, 2003, **1**, 3471–3491.

240 T. F. De Greef, M. M. Smulders, M. Wolffs, A. P. Schenning, R. P. Sijbesma and E. W. Meijer, *Chem. Rev.*, 2009, **109**, 5687–5754.

241 M. Goodman, A. S. Verdini, C. Toniolo, W. D. Phillips and F. A. Bovey, *Proc. Natl. Acad. Sci. U. S. A.*, 1969, **64**, 444–450.

This journal is © The Royal Society of Chemistry 2018

Chem. Soc. Rev., 2018, **47**, 7401–7425 | 7425